4-28-2014

Adsorption, Diffusion and Activity of Polycatalytic Cellulase-Nanoparticle Conjugates

Ranjan Kumar Kamat
University of Connecticut, ranjan.kamat@uconn.edu

Adsorption, Diffusion and Activity of Polycatalytic Cellulase-Nanoparticle Conjugates

Ranjan Kumar Kamat, Ph. D.

University of Connecticut, 2014

Biomass is a sustainable and renewable energy resource that can be converted to liquid transportation fuels. However, conversion of cellulosic biomass into fuels is challenging due to its recalcitrant nature for enzymatic degradation. Inspired by the high efficiency of natural polycatalytic cellulase complex, cellulosome, we aim *to create and investigate artificial cellulosomes with high activity, and systematically evaluate the fundamental principles that underlie their structure, dynamics and catalytic functions.* To achieve our objective, we first studied the free cellulase system and found that it forms unique on-site assembly on cellulose surface which help it to overcome obstacle and regain processivity and thus significantly enhances its hydrolytic activity. This observation clearly suggests that free enzymes also uses complex form to enhance its activity which will help us to identify critical parameters required in a highly efficient artificial cellulase complex. Next, we developed a polycatalytic system consisting of cellulases covalently linked on the surface of colloidal polymers with a magnetic nanoparticle (MNP) core. MNP provides a convenient handle to separate the complex, while the colloidal polymer would serve as a benign scaffold to attach the enzymes. We investigated how the biochemical properties of free fungal cellulase changes on complex formation by studying its adsorption, diffusion and catalytic activity. We also identified the physical properties of scaffold

which influences the catalytic efficiency of cellulase complex. Thus, the present studies address the key challenges in development of artificial cellulosome complex which is important for the economical production of biofuels from non-food sources.

Ranjan Kumar Kamat - University of Connecticut, 2014

Adsorption, Diffusion and Activity of Polycatalytic Cellulase-Nanoparticle Conjugates

Ranjan Kumar Kamat

B.Tech, University of Calcutta, 2005

M.Tech, Indian Institute of Technology Delhi, 2007

A Dissertation

Submitted in Partial Fulfillment of the

Requirement for the Degree of Doctor of Philosophy

at the

University of Connecticut

2014

APPROVAL PAGE

Doctor of Philosophy Dissertation

Adsorption, Diffusion and Activity of Polycatalytic Cellulase-Nanoparticle Conjugates

Presented by

Ranjan Kumar Kamat

Major Adviser……
Dr. Yao Lin

Associate Adviser……
Dr. Rajeswari M Kasi

Associate Adviser……
Dr. Mu-Ping Nieh

University of Connecticut

2014

Acknowledgements

During my graduate career I have been greatly benefitted from the people around me who have been very supportive and encouraging in numerous ways. Most importantly, I would like to thank and express my deepest appreciation to my advisor, Prof. Yao Lin for giving me an opportunity to work in this field and for all of the encouragement and guidance. His encouragement and support for exploring new ideas were invaluable as was his critical review of data, manuscripts and presentations. Besides my advisor, I would also like to thank other members of my advisory committee: Prof. Challa Vijay Kumar, Prof. Rajeswari M. Kasi, Prof. Mu-Ping Nieh and Prof. Jing Zhao who often served in the advisory roles which helped provide direction for this work. I would express my gratitude to Prof. Challa Vijay Kumar with who I had several long discussion which were not only invaluable for this dissertation but also helped me build a strong foundation in biophysical chemistry. I am grateful to Prof. R. M. Kasi for allowing me unconditional access to her laboratory.

I would also like to thank Prof. Changchun Wang and Wangfu Ma (Fudan University, China) for providing the magnetic particles for my research work.

I owe a lot to my group members: Dr. Jing Wang, Dr. Youngkun Yang, Hongwei Xia, Ren, Connor Elliott, Daniel Peck, Xixan and Murali Anuganti who were incredibly supportive and have been nice to me for all these years.

I would like to specially thank YoungHee Chudy for her constant encouragement, help and advice at different stages of my graduate life.

I would also like to thank Carol, Mark Dudley, Marcus Giotto, Rogers, Stephen Daniels, Gary Lavigne and JoAnne Ronzello for training me on instruments and giving their best inputs regarding experimental protocols. In addition, I would like to thank Kim Post, Deb Perko, Nancy, Maria, Shari, Rhonda for helping me with the administrative work.

Finally, I would like to thank my family for their unconditional love, encouragement and patience with my endeavors. I wouldn't have made through graduate school without their support. I would like to specially thank my wife, Anju, for being the constant sources of support, encouragement and love. Last but not the least, my daughter, Kavya, for all the happiness she brought in our life.

Table of Content

List of Figures

List of Tables

Abbreviation and symbols

Abbreviation

CBHI	Cellobiohydrolase I
EGII	Endoglucosidase II
*Tr*Cel7A	*Trichoderma reesei* cellobiohydrolase I
CBD	Cellulose binding domain
CD	Catalytic domain
FPLC	Fast protein liquid chromatography
HPLC	High pressure liquid chromatography
PAA	Polyacrylic acid
PMAA	Polymethylacrylic acid
MNP	Magnetic nanoparticle
TIRF	Total internal reflection fluorescence microscopy
EDC	1-ethyl-3-(3-dimethylaminoyl) carbodimide hydrochloride
FESEM	Field emission scanning electron microscopy
LFCM	Lasser-scanning fluorescence confocal microscopy

Symbol

B	Equilibrium concentration of bound enzymes
F	Equilibrium concentration of free enzymes
N_t	Maximum binding capacity
m	Heterogeneity index
K_A	Mean binding affinity

Chapter 1

Natural and Artificial Cellulase Systems

1.1 INTRODUCTION

Biomass is a sustainable and renewable energy resource that can be converted to liquid transportation fuels.[1, 2] It is estimated that biofuel production in the US will reach 60 billion gallons per year by 2030 while the European Union (EU) aims to supply 25% of transportation fuel through biofuel production by 2030. Currently, sugarcane (in Brazil) and corn (in the US) are used as feedstock for biofuel production but it is not sufficient to supply such huge demand. Thus, lignocellulosic biomass is considered as feedstock for biofuel production since it consists of approximately 75% polysaccharide sugars. However, lignocellulose is highly recalcitrance toward either chemical or enzymatic degradation which makes conversion of biomass to biofuel very difficult.

Plant biomass has evolved as a structurally and chemically complex material to resist degradation of its structural sugars from the microbial and animal kingdoms. The most important factors which contribute to the recalcitrance of lignocellulosic feedstock to chemicals or enzymes are (i) lignin content; (ii) crystallinity of cellulose; (iii) the structural heterogeneity and complexity of cell-wall; (iv) presence of cuticle and epicuticular waxes; (v) the relative quantity of sclerenchymatous tissue and (vi) the arrangement and density of the vascular bundles.[1] These chemical and structural features of biomass significantly hinder liquid penetration and/or enzyme accessibility and activity. At molecular level, cellulose chains are closely packed into a highly crystalline structure. There is strong interchain hydrogen bonding between adjacent chains in a cellulose sheet and weaker hydrophobic interactions between cellulose sheets which arise due to

precise orientation of glucose unit. The hydrophobic face of cellulose sheets also makes crystalline cellulose very resistant to acid hydrolysis because it leads to formation of a dense layer of water near the hydrated cellulose surface. Based on chain arrahgment, native cellulose can be classified into two group cellulose I: cellulose chains are arranged in parallel direction of the long axis of the microfibril; cellulose II: cellulose chains are in antiparrellel position. Cellulose I is the dominant cellulose structure and it can be converted to cellulose II by alkali treatment (mercerization). Studies show that cellulose I actually contain two distinct crystal lattices: cellulose Iα**,** with triclinic symmetry, and cellulose Iβ**,** with monoclinic symmetry. These two forms differ in the organization of their intermolecular hydrogen bonds and lead to further complexity of cellulose structure. The percentage crystallinity of cellulose varies from very low to almost 100% and it depends on cellulose source. However it is clear that cellulose microfibrils are not uniformly crystalline: imperfections in packing or mechanical damage result in a proportion of substrate in which the lattice is disordered or paracrystalline. Considering whole biomass structures, access to the crystalline cellulose cores of microfibrils is restricted by a coating of amorphous cellulose and hemicellulose. The heterogeneous and complex nature of cellulose at both microscopic and macroscopic scale, limits mass-transport for chemical or biochemical catalysts. So a pretreatment step is usually conducted to reduce recalcitrance by depolymerizing and solubilizing hemicelluloses. Pretreatment mainly, converts hemicelluloses to monosaccharides and oligosaccharides, which can be further, hydrolyzed or fermented. Removal of hemicellulose from the microfibrils exposes the crystalline cellulose core for further hydrolysis by cellulase enzymes. For research purposes, purified insoluble, unsubstituted plant celluloses are used as close approximations to native crystalline cellulose but soluble, unsubstituted, mixed linkage glucans soluble, substituted celluloses (carboxymethylcellulose), as

well as soluble cellooligosaccharides and glucosides, are also used to investigate specific aspects of cellulase activity. Generally, Avicel, filter paper or cotton are often used to study the activity or adsorption of cellulases because they are considered representative of highly crystalline cellulose I and are readily available.

Conversion of cellulose to biofuel can be achieved by both chemical and enzymatic treatments; however both systems suffer from certain limitation like chemical methods are efficient but it uses highly concentrated acids under high temperature and pressure which leads to corrosion of equipments and environmental concern. So the current research mainly focuses on development of solid acids which can be reused and also less harmful for both environment and equipments. On the other hand enzymatic degradation is environment friendly but it is less efficient. So the current research is mainly focused on improvement of its catalytic efficiency by different pretreatment methods, protein engineering and development of reusable artificial polycatalytic enzymes system. Thus, enzymatic treatment holds the key of a green, sustainable and renewable energy source.

1.2 Enzymatic Degradation of Cellulose

Enzymatic hydrolysis of cellulose has emerged as one of the most important technology for the conversion of biomass into monomer sugars which can be subsequently fermented to bioethanol. It is very interesting to find that even the digestion of purified native cellulose under laboratory conditions requires concerted action of several enzymes. The interaction among different enzymes, even in relatively simple cellulase systems, is still not well understood and continues to be the primary focus of most work in the field. Cellulase enzymes are secreted by many aerobic and anaerobic microorganisms and based on their taxonomic and ecological diversity, the cellulase systems can be divided into two main categories: non-complexed and complexed.[3]

Non-complexed cellulase systems are mainly secreted by aerobic fungi and bacteria. It comprises of several soluble cellulases and related polysaccharide depolymerases. The complexed systems are secreted by anaerobic bacteria and fungi. The complexed enzyme of some anaerobic bacteria like *Clostridium* spp., are distinct high-molecular-weight protein complexes called cellulosomes.[4] in the following sections the detail properties of non-complexed and complexed cellulase systems have been discussed.

1.2.1 Non-complexed Cellulase Systems

The soft-rot fungi (e.g. *Trichoderma* spp. *Fusarium* spp., *Penicillium* spp., and *Talaromyces emersonii)* are the major non-complexed cellulase producing microorganism. It secretes a combination of endoglucanases and exoglucanases (cellobiohydrolases) into the surrounding medium (**Figure 1.1**). The cellulase system of *T. reesei* is the most studied and has become a paradigm for this group. It comprises of two major cellobiohydrolases, (CBHI and CBHII), two major endoglucanases, (EGI and EGII) and at least two low-molecular weight endoglucanases, EGIII and EGV. The mixture of these enzymes is capable of solubilizing native cellulose. Many other aerobic filamentous fungi, including *Agaricus bisporus*, *Humicola* spp., *Irpex lacteus* and *Sclerotium roysii*, also uses similar cellulase systems.

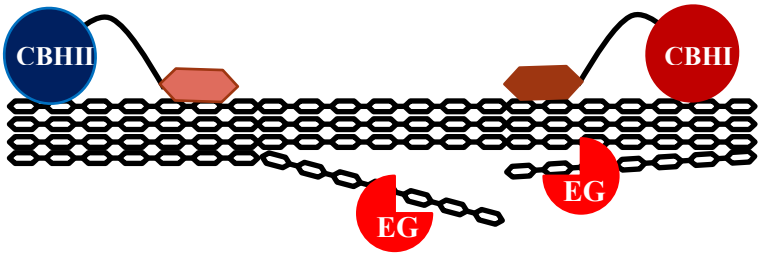

Figure 1.1: Major enzymes of non-complexed cellulase system working on crystalline cellulose.[5]

CBHI is the dominant cellulase of fungi and is capable of completely hydrolyze the highly crystalline *Valonia* cellulose by itself.[6] CBHI is modular in nature, as the catalytic domain is linked via a 6−109-residue polypeptide linker to a smaller cellulose binding module (CBM), which facilitates adsorption to insoluble cellulosic substrates.[7, 8] In cellobiohydrolases, the active site is located within a tunnel that can accommodate 6−10 glucosyl units. and it consist of two glutamate and/or aspartate residues positioned to promote general acid-catalyzed hydrolysis of β-1,4-bonds that link the repeating cellobiose subunits of cellulose chains.[9] The basic biochemical step involve during cellulose hydrolysis by CBHI (**Figure 1.2**) are (i) adsorption to the crystalline regions of the cellulose surface via its CBM domain. (ii) diffusion along the surface till it forms complexes with a cellulose chain end via its catalytic domain, (iii) it releases glucose, cellobiose, or cellotriose during initial hydrolysis event, (iv) and only cellobiose, as it processively moves along the chain, (v) finally, it decomplexes from the cellulose chain then either recomplexes with a cellulose chain or desorbs from the surface.[10] Higher efficiency of CBHI arise due to its processive motion which helps it to overcome the efficiency loss due to diffusion.

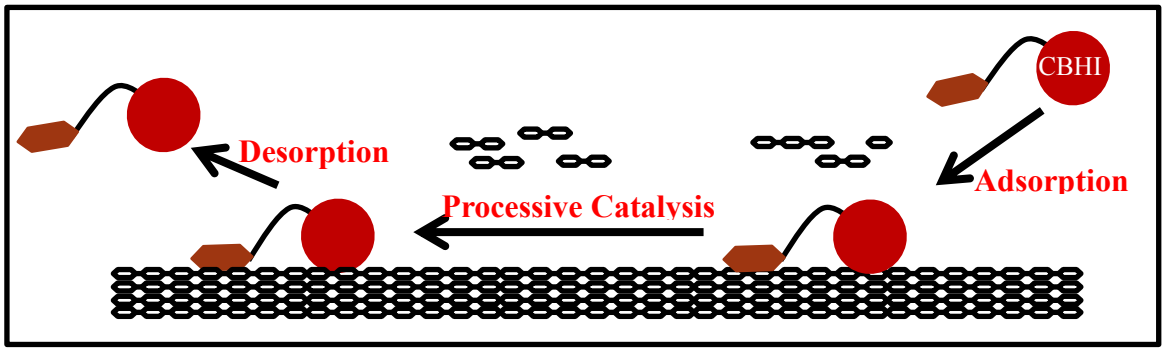

Figure 1.2: Different biochemical steps involve during cellulose hydrolysis by cellobiohydrolase I. [10]

Thus, processive motion is very important for efficient degradation of cellulose.[11] However, the processivity value (Number of catalytic reaction performed during single run) measured for

CBHI on cellulose hydrolysis were more than an order of magnitude lower than the values of intrinsic processivity that were calculated from the ratio of catalytic constant (k_{cat}) and dissociation rate constant (k_{off}). Valjamae et. al proposed that the length of the obstacle free path available for a processive run on cellulose chain limits the processivity of CBHs on cellulose. A recent study, clearly demonstrate that based on cellulose type population of moving and stop CBHI molecules varies.[12, 13] It was observed that movement of CBHI gets halted after performing certain number of catalytic reaction (**Figure 1.3**). And after subsequent jamming of several additional cellobiohydrolase molecules, the blocked CBHI molecules started to move again on the cellulose surface.

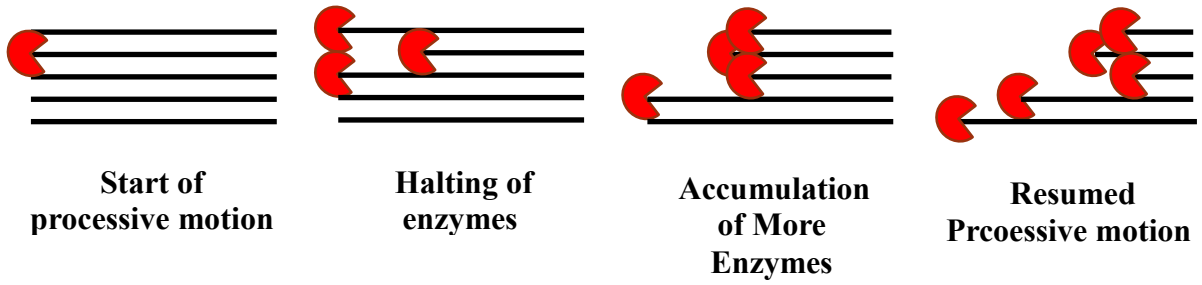

Figure 1.3: Artistic depictions of traffic jam phenomena of cellobiohyrolase I on cellulose surface. [13]

This phenomenon suggests that cellulose has some sites which hinder the processive motion of cellobiohydrolase and the barrier is high enough that a single enzyme molecule is unable to climb over and is therefore halted. Thus, halting of CBHI on cellulose surface significantly reduces its efficiency.[13] Recent studies shows that with the help of companion cellulase enzymes like EG, β-glucosidase etc, CBHI is able toovercome the traffic jam and product inhibition effect. Synergistic interaction among different type of cellulase enzymes helps it to significantly enhance its catalytic efficiency.

1.1.1.1 Synergy among Different Types of Non-complexed Cellulases

Many studies suggest that mixtures of fungal enzymes interact synergistically, i.e. their combined activity on cellulose was greater than the sum of their individual activities. [14]The effect is more pronounced in case of crystalline substrates. Synergy among cellobiohydrolase and endoglucanases is very important and well studies.[14] In endoglucanases, the active site is located within a 3− 5-residue binding site cleft and consist of two glutamate and/or aspartate residues positioned to promote general acid-catalyzed hydrolysis of the β-1,4-bonds.14 The simplest explanation of synergy suggests that the substrate concentration for at least one enzyme is rate-limiting and that the other enzyme overcomes this limitation for its partner. A widely held model for endo-exo synergy describes the sequential interaction of an endoglucanase with cellobiohydrolases, in this case, the rates of hydrolysis of the exo-acting cellobiohydrolases are limited by the availability of cellulose chain ends; the endoglucanase cannot hydrolyse crystalline cellulose efficiently but cleaves bonds at relatively accessible "amorphous regions" to provide sites for cellobiohydrolase attack. Although this general model is widely accepted, but recent finding suggest that the interaction between CBH and EG is more complex than expected. [15] According to Valjamae et.al at optimal enzyme/substrate ratios, the "steady state" rate of synergistic hydrolysis became limited by the velocity of processive movement of CBHI on Cellulose. A processivity value close to the leveling off degree of polymerization of Cellulose was measured for CBHI, suggesting that CBHI cannot pass through the amorphous regions on cellulose and stalls. Thus, they suggest that the mechanism of endo-exo synergism is due to degradation of amorphous regions by EG which avoids the stalling of CBHI and leads to its accelerated recruitment.[15] Synergy among strictly exo-acting cellobiohydrolases can be explained if each enzyme recognizes only one of the two possible stereospecific configurations

of cellobiose residues exposed on the cellulose surface. A second hypothesis is preference of CBHI and CBHII for hydrolysis of celluloses Iα and Iβ, respectively. The degree of synergy can vary with the enzyme:substrate ratio and the form of cellulose substrate used so conditions need to be carefully defined and considered when comparing different experiments. Although, the molecular basis of synergy is still not well understood; but it is an important factor in developing a more advance cellulase system with higher efficiency. Synergistic interactions are highly optimized in case of complexed cellulase system which shows significantly higher catalytic efficiency.

1.1.2 Complexed Cellulase Systems: Cellulosome

The most effective biocatalysts for the degradation of lignocellulose are not a simple mixture of individual cellulases, but a supramolecular array of protein-enzyme complexes, called the cellulosomes.[16, 17] These complexes are found on the surface of anaerobic microbes (Figure 2) which feed on cellulose as the energy source. Cellulosome from C. *thermocellum* is the major and most studies cellulosome but cellulosomes are also produced by other cellulolytic *Clostridium* spp. Cellulosomes consist of a protein scaffold ("scaffoldin") which binds and organizes many cellulolytic enzymes into a very large protein complex (~tens of nanometers in dimensions), wherein the catalytic units are positioned to work in a concerted manner to degrade lignocellulose very efficiently.[18] The assembly of cellulosome is facilitated by the high-affinity recognition between cohesin modules of the scaffoldin subunit and enzyme-borne dockerin modules. Cellulose-specific carbohydrate-binding module (CBM) is another important cellulosomal component, which functions as the major binding factor for specific recognition of polysaccharide substrates. CBMs can reside either in the cellulosomal scaffoldin or enzyme subunits. Furthermore, a number of cellulosomes can cluster into even larger complexes, called

polycellulosomes which are hundreds of nanometers in size and serve as reservoirs for cellulosomes.[19-21] Many factors influence their overall enzymatic activities, but the fundamental characteristic of these large enzyme assemblies is simply their multicatalytic nature. As cellulose deconstruction requires enzymatic reactions that take place on insoluble cellulose surfaces, the adsorption and surface mobility of the enzymatic units play a critical role in the kinetics of the surface reactions. It appears that one major function of polycellulosome is efficient deposition of cellulosomes on cellulose surface and mimicking this mechanism will be essential to engineer highly effective multi-catalytic enzyme systems which can function efficiently even at low enzyme concentrations. Upon adsorption, polycellulosome starts unraveling, depositing its cellulosomes on the cellulose surface (**Figure 1.4**). The highly multivalent nature of the interactions between polycellulosome and cellulose surface is responsible for enhanced adhesion of the catalytic units to the cellulose surfaces. Eventually, cellulosomes dissociate from polycellulosomes and diffuse on cellulose surface to continue the catalytic reactions with their substrates. Mimicking the adsorption and diffusion mechanisms of multicatalytic assemblies of the natural system is the focus of many research works. Specific activities of natural cellulosomes (i.e. activity per unit mass of the enzyme) are more than 10 times higher than a corresponding mixture of individual cellulases.[22-25] Despite the significant advantage of multicatalytic assemblies, it is not practical to directly utilize naturally occurring enzyme complexes in the industrial applications, considering their limited availability (e.g. from slow-growing anaerobic microbes), high purification cost, and extreme complexity. Creating low cost, artificial multicatalytic assemblies with high efficiency is thus an attractive proposition. Recent elegant mechanistic studies of cellulosome-like enzyme assemblies, albeit in the systems with a low degree of complexity consisting of 2~4 catalytic units, suggested that improved surface

adsorption and enhanced cooperativity[23-25] among different catalytic units are two key factors.[26] However, the rationale behind the increased efficiency of the natural catalytic complex is still not clearly understood, and a deeper understanding of their function can lead to the rational design of efficient artificial systems.

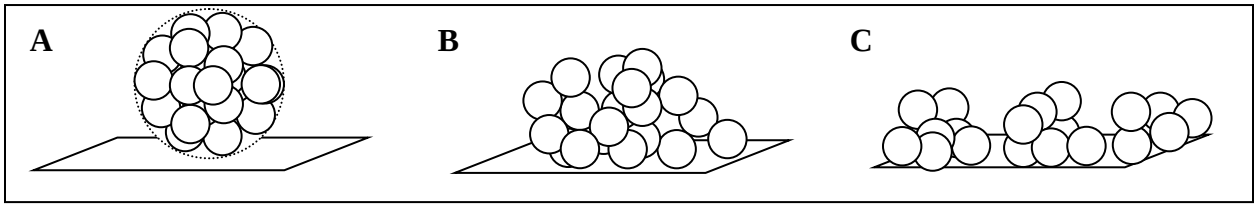

Figure 1.4: Schematic diagram of the interaction of cellulosomes with cellulose. (**A**) A cluster of cellulosomes (polycellulosome) adsorb on the cellulose surface. The spheres are schematic representation of individual enzymatic units in cellulosomes (scaffoldins are omitted for clarity in the diagram). (**B**) Upon adsorption, the cluster changes morphology to provide more contacts between cellulosomes and cellulose surface. (**C**) Individual cellulosomes dissociate from the cluster and continue reaction-coupled diffusions on the cellulose surface.

1.1.3 Nature Inspired Artificial Polycatalytic Cellulase Systems

Activities of natural cellulosomes are an order of magnitude higher than a corresponding mixture of individual cellulolytic enzymes without scaffoldin. Increased activity of Cellulosome has been generally attributed to the proximity of different synergistic enzymes and improved substrate binding in the integrated supramolecular structure of the cellulosome. Inspired by the hydrolytic efficiency of natural cellulosomes, artificial organization of 2-4 cellulolytic enzymes into cellulosome chimeras (e.g. “mini-cellulosomes”) has shown to result in characteristically higher activities on recalcitrant substrates.[27-31] Further extension of the artificial cellulosome concept led to the recent efforts in integrating the industrial cellulases (e.g. produced from Fungi) with a

variety of nanoscaffolds to assemble multi- or poly-catalytic cellulase complexes, that resulted in enhanced activities or stability.[30-36] The cellulosome-inspired complexes were made by immobilization of industrial cellulases on low cost synthetic polymer or nanoparticle scaffolds, and they are technologically attractive due to the simple process involved in the material synthesis, the recyclability of the nanoscaffolds, and the scale-up potential for biorefinery applications. A robust nano-scale platform, such as polymeric nanoparticles, can serve as an analog to the cellulosomal scaffold that holds together individual enzymes in the multimeric complex. This approach uses cellulase enzymes that have already been purified and extensively characterized, therefore bypassing the difficulties in recombinant methods required to engineer cellulosomes. Thelen et. al conjugated cellulase to spherical nanometer-size beads, and characterized the enzymatic activity of the cellulase-nanosphere complex on different substrates and demonstrated that clustering the cellulase on nanospheres results in significant enhancement of enzyme efficiency on insoluble substrates due to increasing enzyme-substrate interactions.[37] It has been also reported that cellulase immobilized onto chitosan microspheres and sponges could be used repeatedly 10 times till its losses 50% of its activity. Similar examples of cellulase immobilized system have been reported in literature.[33-36, 38] A recent studies on clustering of cellulase on streptavidin and CdSe shows improvement in catalytic efficiency upto 7 times compared to mixture of free enzymes. They also reported difference in efficiency based on type of scaffold. [32] These studies clearly suggest that efficiency of cellulase can be improved by complex formation and the physical properties of scaffold plays significant role in improvement in catalytic efficiency.

1.1.4 Motivation, Hypothesis and Specific Aims

Lignocellulose is the most abundant organic substance on the planet, and it is a renewable green energy resource. However, conversion of cellulosic biomass into fuels is challenging due to its recalcitrant nature for enzymatic/chemical degradation. One paradigm for the efficient conversion of biomass to cellulosic products involves a multi-catalytic protein complex, the cellulosome. In cellulosomes, a protein scaffold organizes a variety of functional enzymes into a large complex, wherein different catalytic units work in a concerted manner. Natural cellulosomes exhibit ten times or higher activity than individual cellulolytic enzymes, and this increase in activity has been generally attributed to the proximity of different synergistic enzymes and substrate binding domains in an integrated suprastructure, which facilitates the degradation of the complex network of the lignocellulose. Despite the significant advantages of cellulosomes, they are not practical for industrial applications due to their limited availability, instability for long time periods, and high production cost. Inspired by the hydrolytic efficiency of natural cellulosomes, artificial organization of 2-4 cellulolytic enzymes into cellulosome chimeras (e.g. "mini-cellulosomes") has shown to result in characteristically higher activities on recalcitrant substrates.[27-31] Further extension of the artificial cellulosome concept led to the recent efforts in integrating the industrial cellulases (e.g. produced from Fungi) with a variety of nanoscaffolds to assemble multi- or poly-catalytic cellulase complexes, that resulted in enhanced activities or stability.[30-36] The cellulosome-inspired complexes were made by immobilization of industrial cellulases on low cost synthetic polymer or nanoparticle scaffolds, and they are technologically attractive due to the simple process involved in the material synthesis, the recyclability of the nanoscaffolds, and the scale-up potential for biorefinery applications. This approach uses cellulase enzymes that have already been purified and extensively characterized,

therefore bypassing the difficulties in recombinant methods required to engineer cellulosomes. However, fungal cellulase enzymes were evolved as an individual species and their molecular mechanism are highly co-ordinated to efficiency degrades cellulose. So conversions of fungal cellulase into complex structure will dramatically change its biochemical properties. The change can be either increase its activity or can significantly decrease its activity. Contradictory result in literature can be attributed to these effects. Thus, the objective of the current research is to understand how adsorption, diffusion and activity of fungal cellulase changes on complex formation and also how the physical properties of scaffold affects its activity. Our hypothesis is multivalent nature of artificial cellulase complex will help it to adsorb very efficiently on cellulose surface due to multiple interaction point and will help it to diffuse on cellulose surface uninterruptedly by cleaving multiple cellulose chain simultaneously (**Figure 1.5**). This hypothesis will be tested using well-defined artificial cellulase-polymer coated nanoparticle conjugates where the polymer nanomaterials serve as scaffolds to form artificial cellulosomes. We choose polymer coated magnetic nanoparticle as scaffold as it will help us to completely separate free enzymes from complexed enzymes thus our data will be free from interference from free cellulase. It will also help us to control the surface rigidity and size of the scaffold. So the specific aims of the projects are:

1. *Synthesis and characterization of artificial polycatalytic cellulase-nanoparticle conjugates.*

2. *Investigate and compare the adsorption, diffusion and aactivity of free cellulase and cellulase-nanoparticle conjugates.*

3. *Investigate the effect of physical properties of scaffold on adsorption, diffusion and activity of cellulase-nanoparticle conjugates.*

Rigorous examination of artificially-created, multicatalytic enzyme assemblies would enhance our understanding of how such complexes function in nature. Progress in this area could facilitate the rational design of artificial systems for economical conversion of cellulosic biomass to fuels.

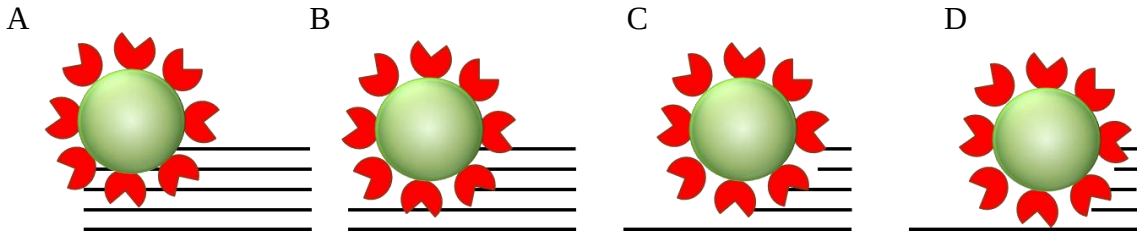

Figure 1.5: Proposed adsorption, diffusion and activity of artificial polycatalytic cellulase-nanoparticle conjugates on cellulose surface. (A) Adsoprtion through multiple interaction points, (B) Depolymerization of several cellulase chains, (C, D), Co-ordinated mobility of cellulase-nanoparticle conjugates on cellulose surface.

1.1.5 Overview of Thesis

In chapter 2, we measured the concentration dependence of CBHI activity and found that productivity (Product produced per molecules in certain time interval) of CBHI increases with increases concentration till certain enzyme concentration and then deceases. We attributed the increase in productivity to minimization of inactive species of CBHI due to formation of on-site assembly. It has been reported that CBHI gets stuck on cellulose surface and loses its activity. Only on aggregation of several CBHI molecules it regains its activity. In our study, change in processivity with increasing concentration and dendence of activity on the surface coverage

further proves this hypothesis. Thus, our study suggest that remarkable efficiency of fungal cellulase arises from its ability to change form from free to complex which helps it to avail the benefits of both high agility of free form and polyvalent nature of complex when it is required.

In chapter 3, we investigated how the adsorption, diffusion and activity of CBHI changes on complex formation. For this study, we first synthesized artificial polycatalytic CBHI-nanoparticle conjugates using carbodiimide coupling reaction. The reaction conditions were optimized to obtain a uniform monodispersion conjugates with ~300 CBHI molecules per particle. CBHI complex shows significantly higher affinity for cellulose than free CBHI due to its multivalent nature. K_d value of CBHI complex is around 200 times smaller than free CBHI indicating multiplepoint of interaction. However, the maximum binding capacity of CBHI complex is significantly lower than free CBHI which may be due to large footprint and electrostatic repulsion of nanoparticles. Activity of CBHI complex was observed to be a function of cellulose/enzyme ratio. At large cellulose/enzyme ratio, CBHI complex shows significantly better activity than free CBHI but at smaller cellulose/enzyme ratio, free enzymes shows better activity. When productivity of CBHI complex was compared with free CBHI, CBHI complex shows much higher productivity which can be attributed to higher local concentration of enzymes. Surface mobility of CBHI complex was measured by TIRF microscopy and analyzed using video tracking software. CBHI complex shows no long range mobility on cellulose surface which contributed to certain extent in its lower activity at high enzyme concentration. We also investigated the effect of scaffold size and polymer shell type on the adsorption and activity of CBHI complex.

In chapter 4, we reported development of EGII based artificial polycatalytic cellulase complexes and compared its adsorption and activity with freely floating EGII. We observed that, although, artificial cellulase complexes are inherently more active but they are unable to compete with natural cellulase at higher concentration due to its large size and very strong binding. Our study suggest that progress in the development of economical biofuel will not only depend on improving the activity of cellulase but also on promoting its accessibility and mobility on cellulose surface.

References

1. Himmel, M. E.; Ding, S.-Y.; Johnson, D. K.; Adney, W. S.; Nimlos, M. R.; Brady, J. W.; Foust, T. D., *Science (Washington, DC, U. S.)* **2007,** 315, (5813), 804-807.

2. Chang, M. C. Y., *Curr. Opin. Chem. Biol.* **2007,** 11, (6), 677-684.

3. Ding, S.-Y.; Liu, Y.-S.; Zeng, Y.; Himmel, M. E.; Baker, J. O.; Bayer, E. A., *Science (Washington, DC, U. S.)* 338, (6110), **2012**, 1055-1060.

4. Bayer, E. A.; Henrissat, B.; Lamed, R., *Biomass Recalcitrance* **2008**, 407-435.

5. Horn, S. J.; Vaaje-Kolstad, G.; Westereng, B.; Eijsink, V. G. H., *Biotechnol. Biofuels, **2012**,* 5, 45.

6. Liu, Y.-S.; Baker, J. O.; Zeng, Y.; Himmel, M. E.; Haas, T.; Ding, S.-Y., *J. Biol. Chem., **2011**,* 286, (13), 11195-11201.

7. Staahlberg, J.; Johansson, G.; Pettersson, G., *Bio/Technology* **1991,** 9, (3), 286-90.

8. Nidetzky, B.; Steiner, W.; Claeyssens, M., *Biochem J,* **1994,** 303 (Pt 3), 817-23.

9. Barnett, C. B.; Wilkinson, K. A.; Naidoo, K. J., *J. Am. Chem. Soc. ,* **2010,** 132, (37), 12800-12803.

10. Fox, J. M.; Levine, S. E.; Clark, D. S.; Blanch, H. W., *Biochemistry ,* **2011***,* 51, (1), 442-452.

11. Igarashi, K.; Koivula, A.; Wada, M.; Kimura, S.; Penttilae, M.; Samejima, M., *J. Biol. Chem.* **2009,** 284, (52), 36186-36190.

12. Igarashi, K.; Uchihashi, T.; Koivula, A.; Wada, M.; Kimura, S.; Penttila, M.; Ando, T.; Samejima, M., *Methods Enzymol.,* **2012,** 510, (Cellulases), 169-182.

13. Igarashi, K.; Uchihashi, T.; Koivula, A.; Wada, M.; Kimura, S.; Okamoto, T.; Penttilae, M.; Ando, T.; Samejima, M., *Science (Washington, DC, U. S.) ,* **2011***,* 333, (6047), 1279-1282.

14. Nidetzky, B.; Claeyssens, M.; Steiner, W., *Biotechnol. Pulp Pap. Ind., Proc* **1996**, 537-542.

15. Jalak, J.; Kurasin, M.; Teugjas, H.; Vaeljamaee, P., *J. Biol. Chem. ,* **2012***,* 287, (34), 28802-28815.

16. Bayer, E. A.; Shoham, Y.; Lamed, R., *Bioenergy* **2008**, 75-96.

17. Ding, S.-Y.; Xu, Q.; Crowley, M.; Zeng, Y.; Nimlos, M.; Lamed, R.; Bayer Edward, A.; Himmel Michael, E., *Curr. Opin. Biotechnol.* **2008,** 19, (3), 218-27.

18. Bayer, E. A.; Lamed, R., *J. Bacteriol.* **1986,** 167, (3), 828-36.

19. Bayer, E. A.; Shimon, L. J. W.; Shoham, Y.; Lamed, R., *J. Struct. Biol.* **1998,** 124, (2-3), 221-234.

20. Leschine, S. B., **1995,** 49, 399-426.

21. Leschine, S. B., CRC Press: Boca Raton, **2004**.

22. Shoham, Y.; Lamed, R.; Bayer, E. A., *Trends in Microbiology* **1999,** 7, (7), 275-281.

23. Fierobe, H. P.; Bayer, E. A.; Tardif, C.; Czjzek, M.; Mechaly, A.; Belaich, A.; Lamed, R.; Shoham, Y.; Belaich, J. P., *Journal of Biological Chemistry* **2002,** 277, (51), 49621-49630.

24. Fierobe, H. P.; Mingardon, F.; Mechaly, A.; Belaich, A.; Rincon, M. T.; Pages, S.; Lamed, R.; Tardif, C.; Belaich, J. P.; Bayer, E. A., *Journal of Biological Chemistry* **2005,** 280, (16), 16325-16334.

25. Koukiekolo, R.; Cho, H. Y.; Kosugi, A.; Inui, M.; Yukawa, H.; Doi, R. H.,. *Applied and Environmental Microbiology* **2005,** 71, (7), 3504-3511.

26. Hammel, M.; Fierobe, H.-P.; Czjzek, M.; Kurkal, V.; Smith, J. C.; Bayer, E. A.; Finet, S.; Receveur-Brechot, V., *J. Biol. Chem.* **2005,** 280, (46), 38562-38568.

27. Fierobe, H.-P.; Bayer, E. A.; Tardif, C.; Czjzek, M.; Mechaly, A.; Belaich, A.; Lamed, R.; Shoham, Y.; Belaich, J.-P., *J. Biol. Chem.* **2002,** 277, (51), 49621-49630.

28. Fierobe, H.-P.; Bayer Edward, A.; Tardif, C.; Czjzek, M.; Mechaly, A.; Belaich, A.; Lamed, R.; Shoham, Y.; Belaich, J.-P., *J Biol Chem* **2002,** 277, (51), 49621-30.

29. Fierobe, H.-P.; Mingardon, F.; Mechaly, A.; Belaich, A.; Rincon, M. T.; Pages, S.; Lamed, R.; Tardif, C.; Belaich, J.-P.; Bayer, E. A., *J. Biol. Chem.* **2005,** 280, (16), 16325-16334.

30. Ho, K. M.; Mao, X.; Gu, L.; Li, P., *Langmuir* **2008,** 24, (19), 11036-11042.

31. Tebeka, I. R. M.; Silva, A. G. L.; Petri, D. F. S., *Langmuir* **2009,** 25, (3), 1582-1587.

32. Kim, D.-M.; Umetsu, M.; Takai, K.; Matsuyama, T.; Ishida, N.; Takahashi, H.; Asano, R.; Kumagai, I., *Small,* **2011***,* 7, (5), 656-664.

33. Hirsh, S. L.; Bilek, M. M. M.; Nosworthy, N. J.; Kondyurin, A.; dos Remedios, C. G.; McKenzie, D. R., *Langmuir ,* **2010,** 26, (17), 14380-14388.

34. Cho, E. J.; Jung, S.; Kim, H. J.; Lee, Y. G.; Nam, K. C.; Lee, H.-J.; Bae, H.-J., *Chem. Commun. (Cambridge, U. K.) ,* **2012***,* 48, (6), 886-888.

35. MacKenzie, K. J.; Francis, M. B., *J. Am. Chem. Soc. ,* **2012***,* 135, (1), 293-300.

36. Liao, H.; Chen, D.; Yuan, L.; Zheng, M.; Zhu, Y.; Liu, X., *Carbohydr. Polym.,* **2010***,* 82, (3), 600-604.

37. Blanchette, C.; Lacayo, C. I.; Fischer, N. O.; Hwang, M.; Thelen, M. P., *PLoS One ,* **2012***,* 7, (8), e42116.

38. Miyauchi, S.; Shimomura, M.; Yamauchi, T., **1999,** 51172 11243951, 19980303., 1999.

Chapter 2

Cooperative Behavior of Processive Cellulase on Semi-crystalline Cellulose Substrate

ABSTRACT

Greater mechanistic understanding of the enzymatic saccharification of cellulosic biomass could help us to enhance its efficiency by modifying reaction or substrate parameters. Herein, we report the unique concentration-dependent reaction kinetics of *Tr*Cel7A on Avicel cellulose substrate. This result indicates that processive cellulase indeed reply on a non-linear cooperative behavior to overcome the obstacle and maximize their processivity on heterogeneous substrate. And the cooperative behavior can be modulated in order to optimize the reaction conditions for increasing the efficiency of cellulose hydrolysis.

2.1 INTRODUCTION

Processive cellulase such as *Trichoderma reesei* cellobiohydrolase I (*Tr*Cel7A) is a two-domain enzyme consisting of a small cellulose-binding domain (CBD) and a catalytic domain (CD).[1] The two domains of the cellulase work synergistically at liquid-solid interfaces and carry out the hydrolytic reactions in a processive manner - i.e., the enzyme remains bound and "slide" along the polysaccharide chain that has been previously separated from the crystalline cellulose lattice.[2,3] Processive cellulases were found to move unidirectionally across the crystalline cellulose surface but stall at various obstacle sites, due to the heterogeneous nature of cellulose surface. Typical processivity values measured for processive cellulases (5-25) were orders of magnitude lower than the values of intrinsic processivity estimated from the ratio of catalytic

constant (k_{cat}, in the range of 1 s^{-1}) and dissociation rate constant (k_{off}, in the range of 10^{-3} s^{-1}).[4] As a k_{off} of 10^{-3} s^{-1} corresponds to a half-life around 10 min, regaining the processivity of jammed cellulases through the way of desorption and re-adsorption is also ineffective. Consequently, these "traffic jams" on obstacles significantly reduce the hydrolytic efficiency of cellulase on cellulose surface.

Interestingly, it has recent been discovered that the subsequent accumulation of multiple processive cellulases behind the blocked enzymes may lead to elimination of the obstacle on the cellulose - a cooperative behavior that potentially recovers the processive motions of some trapped cellulases.[3] While the formation of multicatalytic enzyme complexes (e.g., large cellulosomes produced in some anaerobic bacteria) is known as a powerful mechanism to enhance the efficiency of cellulose hydrolysis, the physical basis of how the temporal clustering of fungal cellulases may reduce the molecular congestion and improve their processivity remains elusive.[5], [6] It is still unclear to which extent this molecular cooperativity may contribute to the overall hydrolytic efficiency of the processive cellulase. In the present chapter, we present a unique concentration-dependent reaction kinetics of *Tr*Cel7A on Avicel cellulose substrate. The results indicate that processive cellulase indeed reply on a non-linear cooperative behavior to overcome the obstacle and maximize their processivity on heterogeneous substrate. And the cooperative behavior can be modulated in order to optimize the reaction conditions for increasing the efficiency of cellulose hydrolysis.

2.2 EXPERIMENTAL

2.2.1 Materials. Cellulase mixture from *Trichoderma reesei* (Celluclast® 1.5 L from Novozymes), β-glucosidase (Novozymes 188), microcrystalline cellulose (Avicel, PH101) and fluorescent labeled cellobiose (4-Methylumbelliferyl β-D-cellobioside) were purchased from

Sigma-Aldrich. All other chemicals were of analytical grade and purchased from Fisher Scientific.

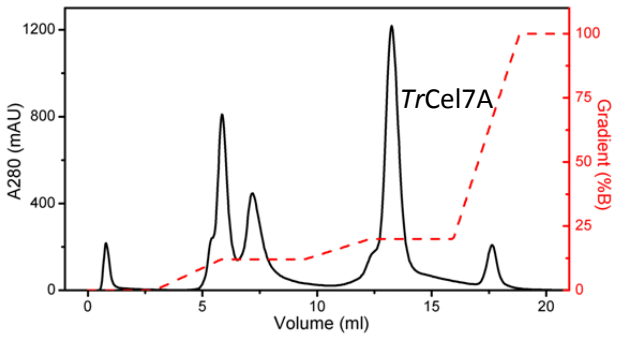

***Figure 2.1*:** FPLC chromatogram of commercial cellulase enzymes. The sample was applied on a Resourse Q column in 20 mM Tris–HCl buffer at pH 8 and eluted by a two-step gradient as indicated in the Figure. (100% B = 100mM NaCl).

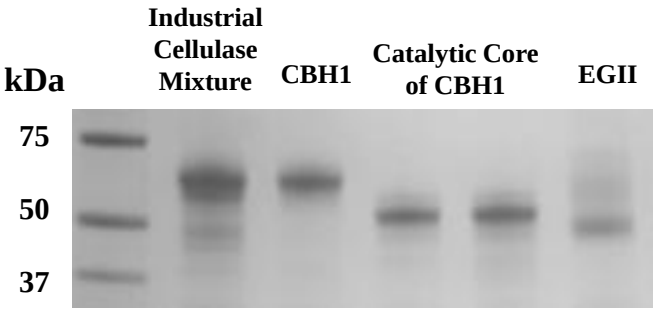

Figure 2.2: The molecular weight of the purified enzymes as determined by SDS-PAGE.

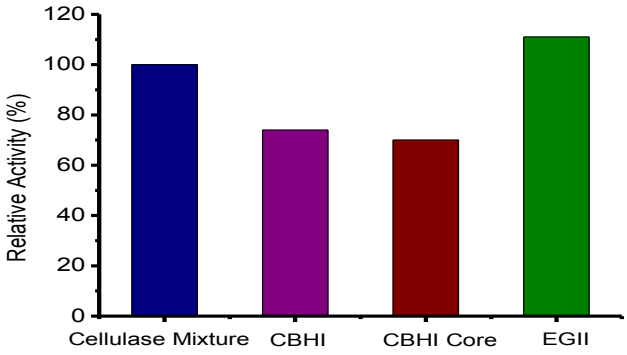

Figure 2.3: Relative specific activities of enzymes against 4-Methylumbelliferyl β-D-cellobioside at 50°C for 10 mins.

2.2.2 Enzyme purification and characterization. *Tr*Cel7A was purified from cellulase mixture as described [34], using GE FPLC equipped with ion exchange columns (**Figure 2.1**). The purity of CBHI and other individual enzymes were verified by their molecular weights using SDS-PAGE ((**Figure 2.2**) and by the very sensitive measurement of the specific activity against small chromogenic substrates at 50 °C (**Figure 2.3**). The extinction coefficient of 78800 $M^{-1}cm^{-1}$ was used to determine the concentration of free CBHI in solution.

2.2.3 Adsorption and activity experiments. 1 ml *Tr*Cel7A solution having different concentration in 50 mM Sodium Acetate at pH 5 was mixed with 5 or 20 mg Avicel in an centrifuge tube and incubated at 37°C temperature on a mixer. At given incubation time (1, 5 and 24 hr), the Avicel was pelleted by centrifugation at 14,000 rpm for 3 min and the supernatant was withdrawn. The concentration of unbound *Tr*Cel7A in the supernatants was determined by measuring A_{280} and the specific activity against 4-Methylumbelliferyl β-D-cellobioside. An aliquot was taken for soluble sugar analysis using HPLC.[35] All experiments were done in triplicate.

2.3 RESULTS AND DISCUSSION

Figure 2.4 shows the reaction kinetics of *Tr*Cel7A (0.01 – 10 μM) on Avicel, a microcrystalline cellulose. The reaction products (Glucose and Cellobiose) were measured using HPLC at specific reaction time and fractional scarification was calculated based on total avicel concentration. Careful examination of the reaction kinetics indicates that the hydrolytic reactions of *Tr*Cel7A almost ceases within five hours at low enzyme concentrations, however, at higher enzyme concentration, reaction was continued even after 24 hrs. In order to measure the continuity of reaction, we calculated the change in reaction rate with time. ***Figure 2.5*** shows that reaction rate

decreases significantly with time which is in accordance with the enzyme kinetics reported for *Tr*Cel7A.[7] The $t_{1/2}$ values of reaction rates at different enzyme/substrate ratio are reported in ***Table 2.1***. The $t_{1/2}$ value indicates that around 0.2 μM added enzyme concentration there is a significant change in enzyme kinetics as $t_{1/2}$ increases by 40%. Now the question is what is the reason of increased efficiency? We believe minimization of inactive species due to formation of on-site assembly is the most likely mechanism for increased catalytic efficiency. At low enzyme concentration most adsorbed *Tr*Cel7A were trapped on the obstacles site on the heterogeneous cellulose surface and thus loses its activity whereas by a cooperative mechanism enzymes are able to maintain its activity at higher enzyme concentration.

Considering the increase in efficiency is due to formation of on-site assembly, then the processivity value should increase with increasing enzyme concentration. The processivity value of *Tr*Cel7A can be estimated by the ratio of processive cut product i.e cellobiose and initial cut product i.e. glucose (***Figure 2.5***).[8] The processivity value obtained in the present study is in the same range as previously reported for *Tr*Cel7A.[8] However, we found a strong correlation between the processivity and enzyme concentration. The processivity value increased with increasing enzyme concentration and shows maxima in the concentration range of 0.2-0.5μM enzyme concentration. The decrease in processivity at higher enzyme/ substrate ratio may arise from the reduction of processive path length available for individual *Tr*Cel7A which could be also responsible for decrease in catalytic efficiency at higher enzyme loading.

A

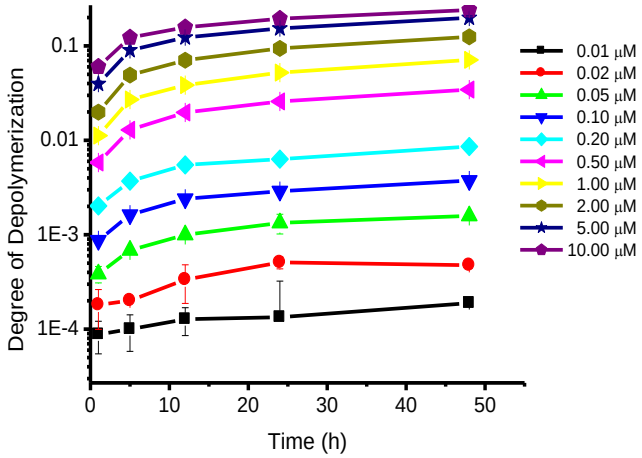

B

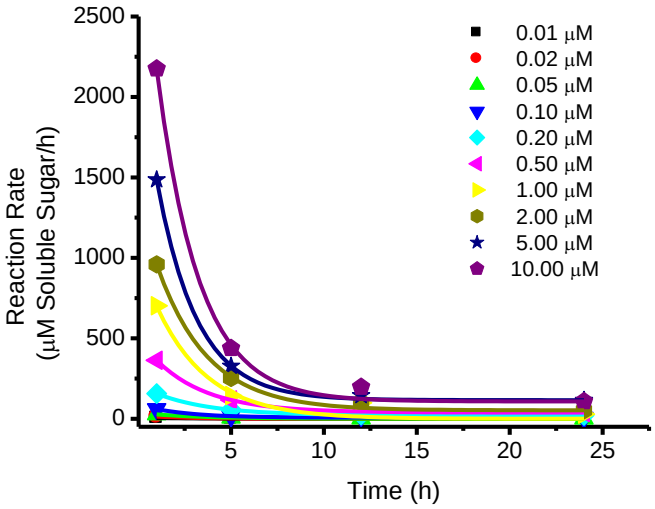

Figure 2.4: (A) Enzyme kinetics and (B) reaction rate with increasing enzyme/substrate ratio using 20 g/l Avicel concentration. The reaction was performed at 37°C in 50mM sodium acetate buffer and amount of soluble sugar was measured using HPLC.

Table 2.1: Half-life of reaction rate at different enzyme concentration.

Enzyme Concentration (μM)	$t_{1/2}$ (hr)
0.01	1.8 ± 0.16
0.02	1.7 ± 0.22
0.05	1.7 ± 0.14
0.10	1.9 ± 0.39
0.20	**3.3** ± 0.11
0.50	2.4 ± 0.04
1.00	2.4 ± 0.77
2.00	2.4 ± 0.22
5.00	2.4 ± 0.08
10.00	1.8 ± 0.19

As the probability of two enzymes coming in close proximity depends on the surface coverage of enzyme, the formation of on-site assembly should be independent of total enzyme concentration in the solution but will be strongly dependent on the surface coverage. So we first measured the surface bound enzyme concentration and calculated fractional surface coverage at particular enzyme/substrate ratio. *Tr*Cel7A shows very fast adsorption and reaches saturation within few minutes at lower enzyme concentration and within an hour at high enzyme concentration. Thus surface bound enzyme concentration remains constant throughout the reaction time. ***Figure 2.6*** shows the turnover number of *Tr*Cel7A i.e. amount of product produced by 1 μM *Tr*Cel7A in one hour, at different surface coverage. There is significant increase in turnover number of *Tr*Cel7A with increasing enzyme/substrate ratio and reaches maxima around 0.5-0.6 fractional surface coverage. The appearance of peak at similar surface coverage for different avicel concentration further supports our hypothesis that increase in catalytic efficiency is due to formation of on-site assembly.

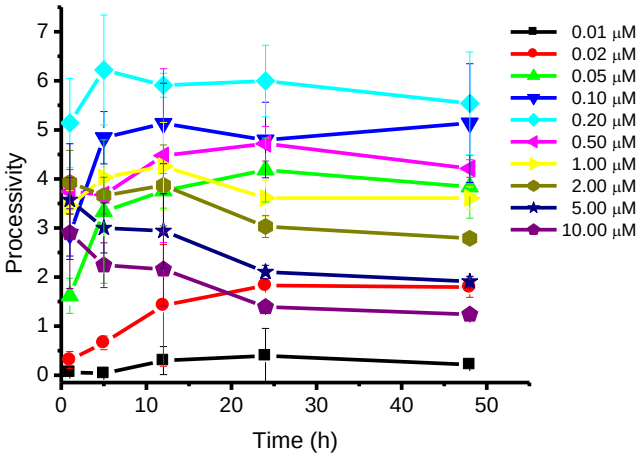

Figure 2.5: Apparent processivity of CBHI with increasing enzyme/substrate ratio. The reaction was performed at 37°C in 50mM sodium acetate buffer and apparent processivity was calculated by the ratio of cellobiose and glucose released during specific reaction time.

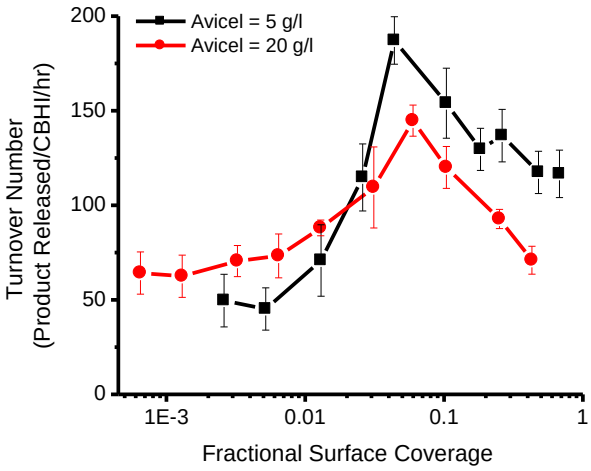

Figure 2.6: Change in productivity of CBHI with increasing surface coverage. The productivity was calculated by dividing the total soluble sugar concentration to actual surface bound enzyme concentration.

To investigate the effect of product inhibition on reaction rate and turnover number at very higher enzyme concentration, activity assay was performed using β-glucosidase which converts cellobiose into glucose. No significant change in total product concentration was observed with or without β-glucosidase which suggests that product inhibition is not the dominant factor in reducing the reaction rate and turnover number at higher enzyme concentration. Hence, reduction in catalytic efficiency and processivity at higher enzyme concentration can be associated with the minimization of processive path length available for individual *Tr*Cel7A molecules. The optimum surface coverage for maximum catalytic efficiency is significantly lower than 1 which indicates that *Tr*Cel7A is mobile species on cellulose surface and thus covers significantly large area than its size. At optimum enzyme concentration, the surface coverage of enzyme is sufficient to form on-site assembly but low enough to provide sufficient space for individual *Tr*Cel7A molecules to move on the cellulose surface. At higher surface coverage, although *Tr*Cel7A is able to form on-site assembly but the mobility of individual *Tr*Cel7A molecules get restricted and hence it shows lower average processivity and activity.

Change in biochemical properties of *Tr*Cel7A on increasing enzyme concentration suggests that molecular mechanism of *Tr*Cel7A on heterogeneous cellulose substrate is different than previously hypothized. It has been reported that *Tr*Cel7A can achieve more than 90% degradation in case of homogenous cellulose like bacterial cellulose which is 100% crystalline, but in case of Avicel maximum degradation percentage is only 50%. The decrease in catalytic efficiency can be associated with heterogeneous nature of avicel. At very low enzyme concentration, individual *Tr*Cel7A gets trapped on cellulose surface and loses its activity (**Figure 2.8A**). At very high concentration as there is shorter chain length it also reduces the efficiency of *Tr*Cel7A by restricting its surface mobility (**Figure 2.8C**). However, at an intermediate enzyme

concentration range, there is sufficient space for mobility so that enzymes can accumulate on a restriction site and by some short of cooperative mechanism overcome the obstacle (**Figure 2.8B**). By this cooperative mechanism majority of *Tr*Cel7A are able to maintain its activity for very long reaction time and thus significantly enhances the efficiency of saccharification process.

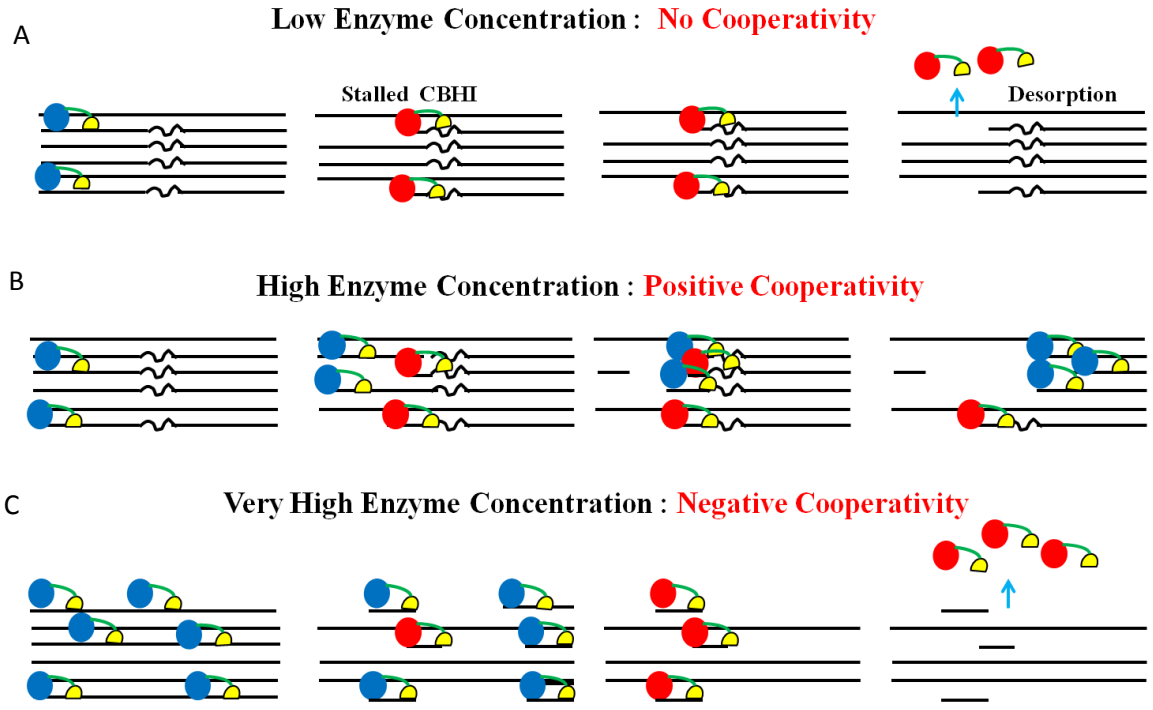

Figure 2.8: Schematic shows the processive motion of *Tr*Cel7A at different enzyme/substrate concentration. Formation of inactive enzyme species reduces the overall productivity of the system. Arrow indicates direction of motion of *Tr*Cel7A. Inactive enzymes become active only after dissociating into bulk solution**.**

In conclusion, the appearance of maxima in catalytic efficiency, processivity and turnover number clearly indicates change in reaction kinetics of *Tr*Cel7A in specific concentration range. The analysis of processivity and turnover number suggest that minimization of inactive species due to formation of on-site assembly is the likely mechanism for improvement in catalytic

efficiency. Thus, we can say that remarkable efficiency of fungal cellulase arises from its ability to change form from free to complex which helps it to avail the benefits of both high agility of free form and polyvalent nature of complex when it is required.

References

1. Staahlberg, J.; Johansson, G.; Pettersson, G., *Bio/Technology* **1991,** *9* (3), 286-90.

2. Igarashi, K.; Koivula, A.; Wada, M.; Kimura, S.; Penttilae, M.; Samejima, M., *J. Biol. Chem.* **2009,** *284* (52), 36186-36190.

3. Igarashi, K.; Uchihashi, T.; Koivula, A.; Wada, M.; Kimura, S.; Okamoto, T.; Penttilae, M.; Ando, T.; Samejima, M., **2011,** *333* (6047), 1279-1282.

4. Kurasin, M.; Vaeljamaee, P., *J. Biol. Chem.* **2011,** *286* (1), 169-177.

5. Bayer, E. A.; Belaich, J.-P.; Shoham, Y.; Lamed, R., *Annu. Rev. Microbiol.* **2004,** *58*, 521-554.

6. Bayer, E. A.; Henrissat, B.; Lamed, R., *Biomass Recalcitrance* **2008**, 407-435.

7. Turon, X.; Rojas, O. J.; Deinhammer, R. S., *Langmuir* **2008,** *24* (8), 3880-3887.

8. Fox, J. M.; Levine, S. E.; Clark, D. S.; Blanch, H. W., *Biochemistry* **2011,** *51* (1), 442-452.

Chapter 3

Adsorption and Hydrolytic Activity of Polycatalytic Cellulase Nano-complex on Cellulose

ABSTRACT

The formation of polycatalytic enzyme complexes may enhance the effectiveness of enzymes due to improved substrate interaction and synergistic actions of multiple enzymes in proximity. Much effort has been made to develop highly efficient polycatalytic cellulase complexes by immobilizing cellulases on low-cost polymer or nanoparticle scaffolds, aiming at their potential applications in biomass conversion to fuels. However, some key cellulases carry out the hydrolytic reaction on crystalline cellulose in a directional, processive manner. A large, artificial polycatalytic complex is unlikely to undergo a highly coordinated motion to slide on cellulose surface as a whole unit. The mechanism underlying the activity enhancements observed in some artificial cellulase complexes and the limit of this approach remain elusive. Herein, we report the synthesis of polycatalytic cellulase complexes bound to colloidal polymer nanoparticles with a magnetic core, and describe their unique adsorption, hydrolytic activities and motions on cellulose. The polycatalytic clusters of cellulases on colloidal polymers show increased rate of hydrolytic reactions on cellulose, but this was observed mainly at relatively low cellulase-to-cellulose ratios. Enhanced efficiency is mainly attributed to increased local concentrations of cellulases on the scaffolds and their polyvalent interactions with cellulose. However, once bound, the polycatalytic complexes can only carry out reactions locally and not capable of relocating to new sites rapidly due to their lack of long-range surface mobility and their extremely tight binding. The development of highly optimized polycatalytic complexes may

arise by developing novel nano-scaffolds that induce concerted motion of the complex as a whole.

3.1 INTRODUCTION

One key challenge in converting biomass to fuels is the recalcitrant nature of cellulosic materials against chemical and enzymatic degradation.[1-5] Natural celluloses (e.g. in plant cell walls) are made of water-insoluble, semi-crystalline polysaccharide polymers stabilized by extensive intra- and inter-chain hydrogen bonds, which provide resistance to hydrolysis. To enhance the efficiency of enzymatic hydrolysis of cellulose, much effort has been made on improving the biological activities of individual cellulases by protein engineering and the design of cellulase cocktails consisting of multiple cellulases and helper enzymes for synergistic actions on recalcitrant cellulose.[6-8] On the other hand, the multi-catalytic enzyme complexes found in some anaerobic bacteria, called cellulosomes, conduct efficient hydrolysis of recalcitrant cellulose. [9-12] Cellulosomes consist of a protein scaffold "scaffoldin" to organize 6-14 enzyme units into a large catalytic assembly, wherein different catalytic units work in a concerted manner.[9-12] Activities of natural cellulosomes are an order of magnitude higher than a corresponding mixture of individual cellulolytic enzymes in the absence of scaffoldin. Increased activity of cellulosome has been generally attributed to the proximity of different synergistic enzymes and improved substrate binding in the integrated supramolecular structure of the cellulosome. Inspired by the remarkable efficiency of natural cellulosomes, artificial organization of 2-4 cellulolytic enzymes into cellulosome chimeras (e.g. "mini-cellulosomes") has shown to result in characteristically higher activities on recalcitrant substrates.[13-15] Further extension of the artificial cellulosome concept led to the recent efforts in integrating the industrial cellulases (e.g. produced from Fungi

rather than bacteria) with a variety of nanoscaffolds to assemble multi- or poly-catalytic cellulase complexes, which resulted in enhanced activities or stabilities. [16-23]

The cellulosome-inspired complexes were made by immobilization of industrial cellulases on low cost synthetic polymer or nanoparticle scaffolds, and they are technologically attractive due to the simple process involved in the material synthesis, the recyclability of the nanoscaffolds, and the scale-up potential for biorefinery applications. Unlike the cellulolytic enzymes in cellulosomes, the industrial cellulases such as *Trichoderma reesei* cellobiohydrolase I (CBHI) are produced by fungi. Many of these fungal cellulases have evolved into a two-domain structure, consisting of a catalytic domain (CD) and a cellulose binding domain (CBD) connected by a peptide linker.[24-29] The cellulases such as CBHI often carry out the hydrolytic reactions in a processive manner – i.e., the enzyme remains bound and "slides" along the polysaccharide chain that has been previously separated from the crystalline cellulose lattice.[30-32] A large, artificial polycatalytic complex consisting of tens to hundreds of immobilized enzyme units is unlikely to undergo a highly coordinated motion to slide on cellulose surface as a whole unit. If polycatalytic complexes show activity enhancements, then what are the mechanisms underlying such behavior? This is a critical question need to be addressed before artificial cellulosomes can be rationally designed to achieve maximal hydrolytic efficiency.

To address this question in the current study, we synthesized polycatalytic cellulase complexes with artificial scaffold nanomaterials, examined their adsorption and hydrolytic activities on cellulose, and compared their performance to the corresponding cellulases in their free state. We identified specific ranges of reaction conditions (e.g. low feeding enzyme-to-substrate ratios), in which the artificial polycatalytic cellulase complexes have significant advantages over freely

dispersed cellulases. The study shows that the enhanced hydrolytic efficiency is attributed to increased local concentrations of cellulases on the scaffolds and their polyvalent interactions with cellulose, particularly at low enzyme loadings on the substrate. Current results bring one step closer to the rational design of artificial cellulosomes and overcome the current bottleneck in the use of recalcitrant biomass for the economic production of biofuels.

3.2 EXPERIMENTAL

3.2.1 Materials. Cellulase mixture from *Trichoderma reesei* (Celluclast® 1.5 L from Novozymes), β-glucosidase (Novozymes 188), glucose oxidase, horseradish peroxidase, papain, microcrystalline cellulose (Avicel, PH101) and 4-methylumbelliferyl β-D-cellobioside were purchased from Sigma-Aldrich. All other chemicals were of analytical grade and purchased from Fisher Scientific. CBHI was purified from cellulase mixture as described,[46] using GE FPLC equipped with ion exchange columns. The purity of CBHI and other individual enzymes were verified by their molecular weights using SDS-PAGE and by the very sensitive measurement of the specific activity against small chromogenic substrate 4-methylumbelliferyl β-D-cellobioside at 50 °C.[36] (**Figure 3.1**) The extinction coefficient of 78800 $M^{-1}cm^{-1}$ was used to determine the concentration of CBHI in solution.[46]

3.2.2 Synthesis of MNPs. In the synthesis of MNPs with a core size of ~200 nm, 1.350 g of $FeCl_3 \cdot 6H_2O$, 3.854 g of $NH_4 \cdot Ac$ and 0.4 g of sodium citrate were dissolved in 70 mL of ethylene glycol. The mixture was stirred vigorously for 1 h at 170 ^oC to form a homogeneous black solution, transferred into a Teflon-lined stainless-steel autoclave (100 mL capacity) and incubated at 200 ^oC for 16 h. The black product was washed with ethanol and separated from the solvent by using a magnet. The washing and separation steps were repeated for several times. The final product was dispersed in ethanol for further use. In the synthesis of MNPs with a core

size of ~100 nm, 1.08 g of $FeCl_3 \cdot 6H_2O$, 2.4 g of NaAc and 0.25 g of sodium citrate were dissolved in 20 mL of ethylene glycol. The mixture was stirred vigorously for 0.5 h at room temperature to form a homogeneous dark red solution, transferred into a Teflon-lined stainless-steel autoclave (50 mL capacity) and incubated at 200 ^oC for 20 h. The washing and separation steps were the same as those in the synthesis of 200-nm MNPs.

3.2.3 Modification of MNPs with MPS. Modification of MNPs with MPS was achieved by adding 40 mL of ethanol, 10 mL of deionized water, 1.5 mL of $NH_3 \cdot H_2O$ and 0.3 g of MPS into the MNPs ethanol suspension and vigorously stirring the mixture for 24 h at 60 ^oC. The obtained product was separated by using a magnet and washed with ethanol to remove excess MPS. The resultant MNP-MPS nanoparticles were dried in a vacuum oven at 40 ^oC till constant weight.

3.2.4 Synthesis of MNP-PAA and MNP-PMAA core/shell particles. Coating PAA or PMAA layer onto MNP-MPS nanoparticles was performed by distillation-precipitation polymerization of AA or MAA in acetonitrile, with MBA as the cross-linker and AIBN as the initiator. Typically, 200 mg of MNP-MPS seed nanoparticles were dispersed in 160 mL acetonitrile in a dried 250 mL single-necked flask, and sonicated for 10 min. A mixture of 0.8 mL of AA or MAA, 89 mg of MBA and 20 mg of AIBN were added to the flask to initiate the polymerization. The flask was submerged in a heating oil bath, and attached with a fractionating column, Liebig condenser, and a receiver. The reaction mixture was heated from ambient temperature to the boiling state within 30 min and the reaction was ended after about 80 mL of acetonitrile was distilled from the reaction mixture (in about 1 h). The MNP-PAA or MNP-PMAA were collected by magnetic separation and washed with ethanol to remove excess reactants and the polymer nano-spheres (without a MNP core) from the side reactions.

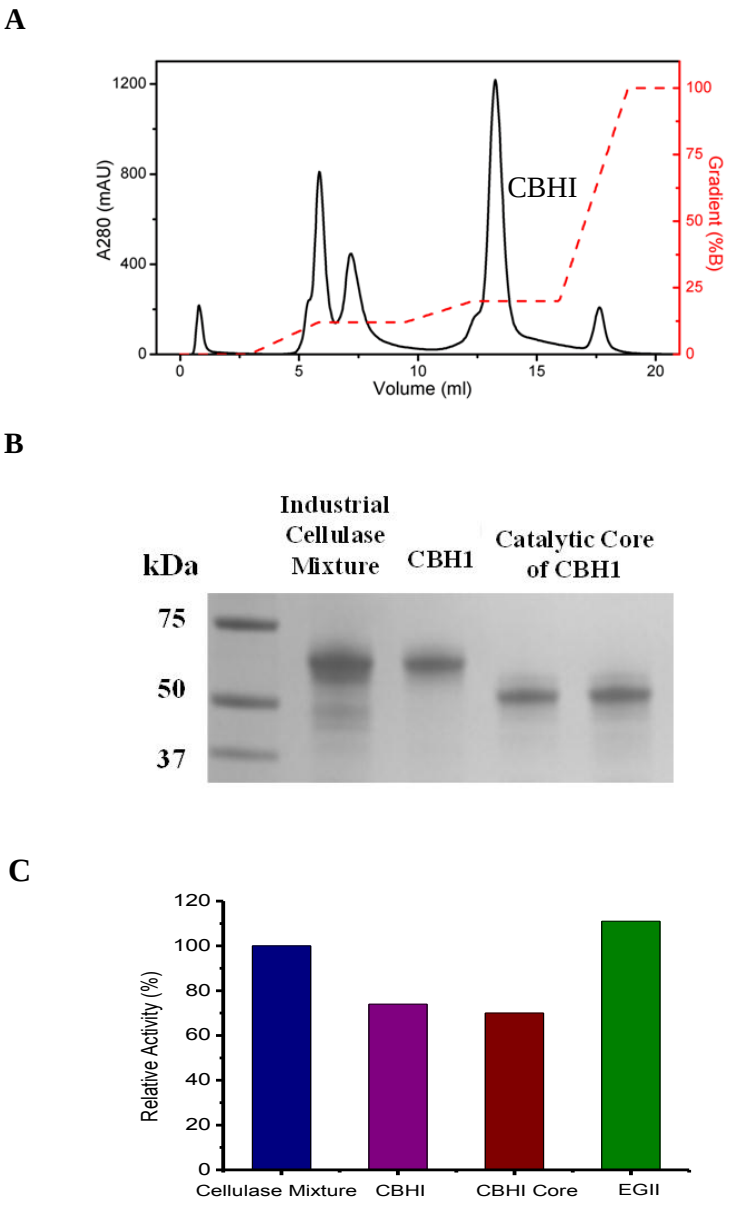

Figure 3.1 : (**A**): FPLC chromatogram of a mixture of cellulase enzymes (Celluclast 1.5L from Novozymes), using GE Resource Q column. (**B**) SDS-PAGE of individual cellulases after purification. (**C**) Relative specific activities of purified enzymes against 4-methylumbelliferyl β-D-cellobioside in 50 mM sodium acetate at 50°C.

3.2.5 Conjugation of cellulase to MNP-PAA or MNP-PMAA particles. CBHI was conjugated to MNP-PAA or MNP-PMAA using 1-ethyl-3-(3-dimenthylaminopropyl) carbodiimide

hydrochloride (EDC) and *N*-hydroxysulfosuccinimide (Sulfo-NHS) coupling chemistry.[35] For conjugation, MNP-PAA or MNP-PMAA solutions were prepared in 0.50M MES buffer at pH 6, with a concentration around 10^{11} particles/ml. 2 mg of EDC and 2 mg Sulfo-NHS were then added into 1 ml of particle suspension, and the solution incubated at room temperature with mixing for 10 min. The activated particles were separated from the solution by a magnetic rack, washed, and added into 2 mg/ml CBHI solution in 12 mM PBS buffer at pH 7.4. The mixture was incubated at room temperature in a rotator for 6 hr followed by washing with 5 mM Tris-HCl buffer for five times to remove unbound proteins. The concentration of CBHI bound to the particles was calculated by comparing the specific activity against 4-methylumbelliferyl β-D-cellobioside in 50 mM sodium acetate at 50 °C with that of the CBHI solutions with the known concentration. (**Figure 3.2**).

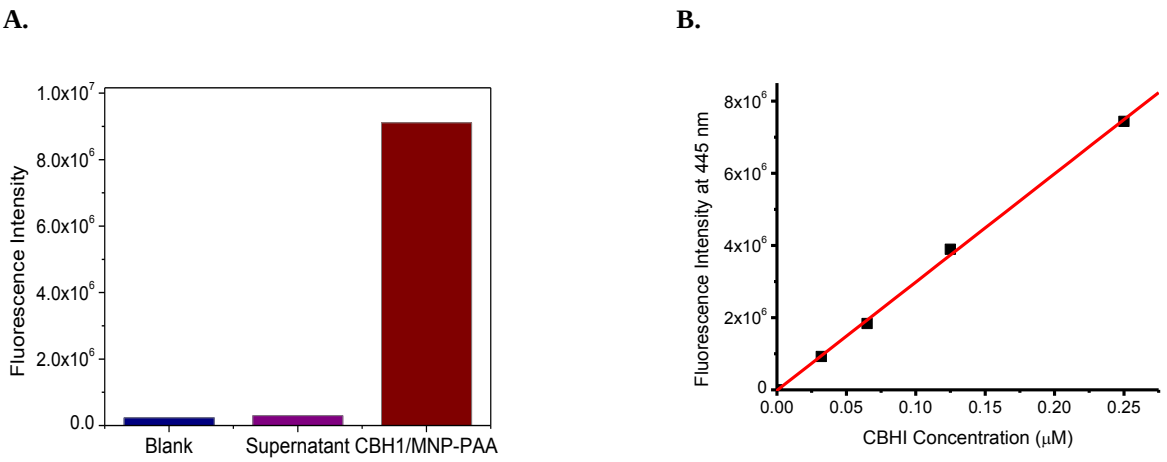

Figure 3.2: (**A**) Measured fluorescence intensity of the buffer, supernatant and CBHI/MNP-PAA complexes after incubated with 4-methylumbelliferyl β-D-cellobioside in 50 mM sodium acetate at 50°C for 10 min. Excitation and emission were set at 365 nm and 445 nm, respectively. (**B**) Correlation between the concentration of CBHI and their activity against 4-methylumbelliferyl β-D-cellobioside.

3.2.6 Adsorption and activity experiments for CBHI. 1 ml CBHI solution in 5 mM Tris-HCl at pH 6.5 was mixed with 20-60 mg Avicel in a centrifuge tube and incubated at 37°C temperature on a mixer. At given incubation time, the Avicel was pelleted by centrifugation at 14,000 rpm for 3 min and the supernatant was withdrawn. The concentration of unbound CBHI in the supernatants was determined by measuring A_{280} and the specific activity against 4-methylumbelliferyl β-D-cellobioside. An aliquot was taken for reducing sugar analysis based on the glucose oxidase (GOX) / horseradish peroxidase (HRP) method and using HPLC.[22, 47] All experiments were done in triplicate.

3.2.7 Adsorption and activity experiments for CBHI/MNP-PAA or CBHI/MNP-PMAA complexes. 1 ml CBHI or CBHI/MNP-PAA or CBHI/MNP-PMAA solution in 5 mM Tris-HCl at pH 6.5 was mixed with 20-60 mg Avicel in a centrifuge tube and incubated at 37°C temperature on a mixer. At given incubation time, a tube was removed from the mixer and put on a rack for 5 min to let the Avicel sediment. Due to their small sizes, the unbound CBHI/MNP-PAA or CBHI/MNP-PMAA remained fully suspended in solution (up to hours) and were pipetted out to separate unbound enzyme complexes from the Avicel. The concentration of absorpted CBHI complexes on Avicel was then determined by comparing the specific activity against 4-methylumbelliferyl β-D-cellobioside with that of stock solution with predetermined amount of CBHI. The suspension of unbounded enzyme complexes were then pelleted by centrifugation at 14,000 rpm for 3 min and the supernatant was withdrawn to determine the concentration of reducing sugars. Adsorption isotherms were determined with 20 mg/ml Avicel.

3.2.8 Surface mobility of CBHI complexes on cellulose thin film studied by TIRF microscopy. Cellulose films (~ 50 nm) were prepared by spin coating of 5 wt % cellulose solution in 1-ethyl 3-methyimidazolium acetate on pre-cleaned coverslip.[48-50] (**Figure 3.3**). The coverslip was placed on a glass slide with the cellulose film facing inward, and affixed by double-side tapes to leave a small gap between the film and the surface of the glass slide. A dilute solution of FITC tagged CBHI/MNP-PMAA complexes (~50 µL) was then introduced into gap and in contact with the cellulose film. The interface between the complex solution and the cellulose thin film was focused and imaged using a Nikon TIRF microscope equipped with an oil immersion TIRF lens (1.49 NA, 100X, Nikon) and an Andor 897 iXon EMCCD camera. Sample environment was maintained at a temperature of 37 ± 3 °C using an environmental chamber and TIRF images were taken at an interval of 5-30 second. Image analysis was performed by using NIH ImageJ software, and the surface mobility of complexes was analyzed by using CISMM Video Spot Tracker program.

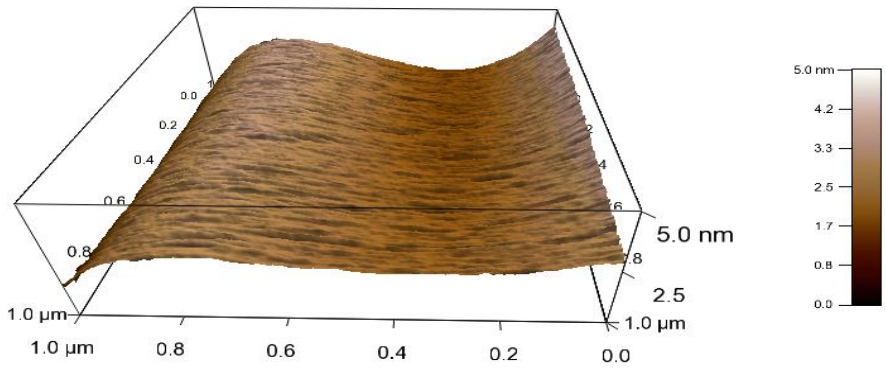

Figure 3.3: AFM image of a cellulose thin film casted on a cover slip. The film was prepared from spinning coating a solution of dissolved Avicel (5 wt%) in 1-ethyl 3-methylimidazolium.

The film was washed by DI water for several times, immersed in buffer for 5 hr, and annealed at 80°C for 30 min.

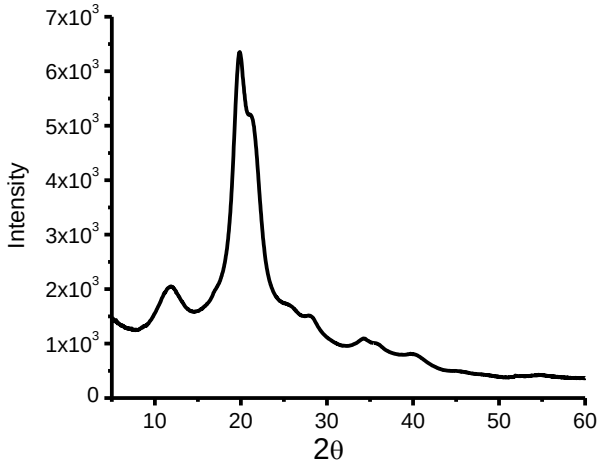

Figure 3.4: X-ray diffraction pattern of regenerated cellulose films.

3.3 RESULTS AND DISCUSSIONS

3.3.1. ***Synthesis of Polycatalytic Cellulase Complexes on Colloidal Polymers with a Magnetic Core.*** Industrial cellulolytic enzymes produced from *Trichoderma reesei* (Novozyme Celluclast®, purchased from Sigma-Aldrich) were purified to homogeneity by GE FPLC AKTA Purifier equipped with ion-exchange columns (see supplemental materials, **Figure 3.1**). The major cellulolytic enzymes (e.g., cellobiohydrolase I (CBHI) and endoglucoisidase II (EGII)) were identified based on their molecular weights and their specific activities (**Figure 3.1**). To unambiguously determine the effect of polycatalytic structures on the hydrolytic efficiency on cellulose, cellulase complexed with the polymer scaffolds are to be completely separated from free enzymes and quantified under the experimental conditions. To address this challenge, we developed a polycatalytic system consisting of cellulases covalently linked on the surface of

colloidal polymers with a magnetic nanoparticle (MNP) core. The MNP-polymer core-shell structures were synthesized through encapsulating γ-methacryloxypropyltrimethoxysilane (MPS) modified Fe_3O_4 nanocrystal clusters with crosslinked hydrophilic polymer shell (**Figure 3.5A**) using the method we previously reported. [33,34] MNP provides a convenient handle to separate the complex, while the colloidal polymer would serve as a benign scaffold to attach the enzymes. In the approach, MNPs with diameter of 200±30 nm were first prepared by a solvothermal process at 200˚C and modified with MPS on the surface. A one-step distillation-precipitation polymerization (DPP) of acrylic acid (AA) or methylacrylic acid (MAA) with *N*, *N'*-methyl-enebisacrylamide (MBA) was used to prepare well-defined core-shell structure with high magnetization susceptibility and large surface density of carboxyl groups (**Figure 3.5B**). The polymer shell thickness and the degree of crosslinking were controlled by adjusting the feeding amount of AA or MAA monomers, MBA crosslinker and 2, 2'-azobisisobutyronitrile (AIBN) initiator. MNP-PAA and MNP-PMAA with a MNP core of 200±30 nm in diameter and a polymer shell of 30±10 nm in thickness and 10% crosslinking were prepared as the scaffold materials.

The carboxyl groups of the PAA and PMAA were then activated for conjugation of cellulase by standard carbodiimide coupling chemistry to produce cellulase/MNP-PMAA and cellulase/MNP-PAA complexes.[35] The complexes are separated from unbound enzymes within 30 seconds by a standard magnetic separation rack. The surface densities of CBHI on MNP-PMAA or MNP-PAA particles were measured by an enzymatic assay using 4-methylumbelliferyl-β-D-cellobioside as the fluorescent soluble substrate[36] (**Figure 3.2**). The reaction conditions were optimized to obtain CBHI complex containing around ~300 enzymes per complex for the initial tests. TEM and Dynamic light scattering (DLS) data were used to determine the size

distributions of the particles after enzyme conjugation (**Figure 3.5C**), and there was no aggregation. These polycatalytic cellulase-particle complexes were then used as the model system to evaluate polycatalytic effects, as they are free of contributions from unbound enzymes.

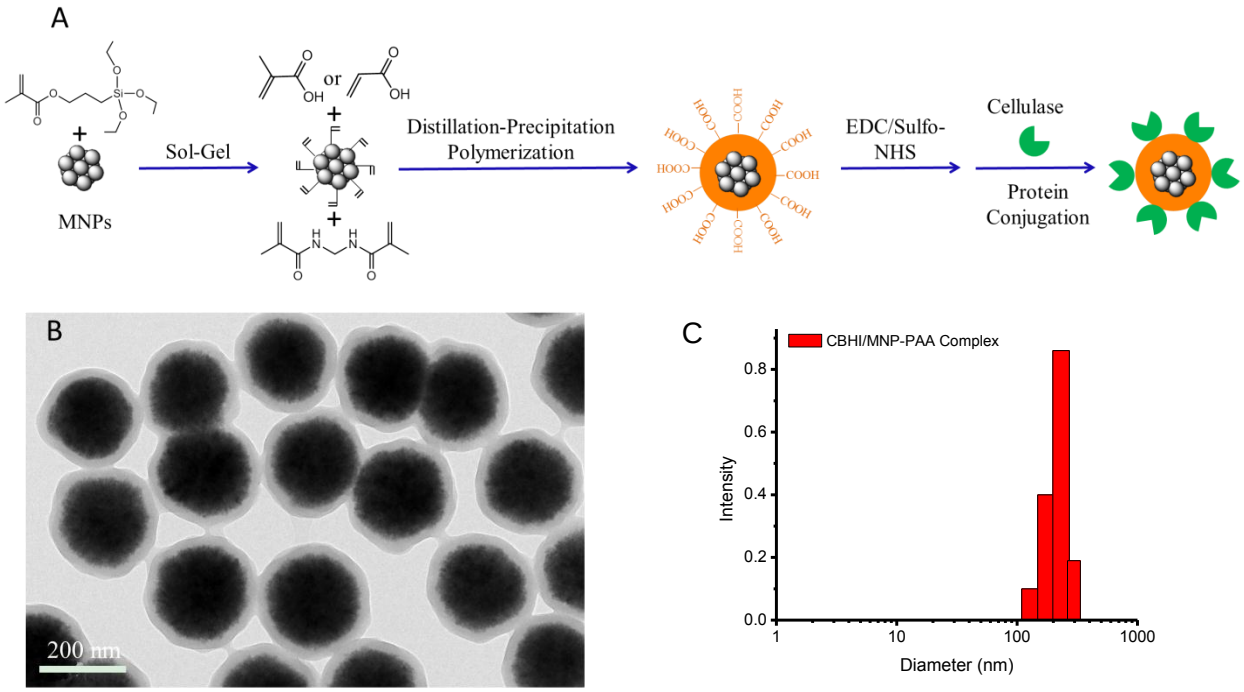

Figure 3.5: (**A**) Schematic of the synthesis of MNP-PAA or MNP-PMAA core-shell particles and the formation of polycatalytic complexes by conjugation of cellulases on the surface of the particle, (**B**) The representative TEM image of the CBHI/MNP-PAA complexes, and (**C**) the distribution of their hydrodynamic radius measured by dynamic light scattering.

3.3.2 Adsorption and Reactions of Polycatalytic CBHI Complexes on Cellulose. CBHI is the dominant cellulase of fungi and is capable of completely hydrolyzing the highly crystalline *Valonia* cellulose by itself.[6,37,38] Therefore, we focused on the polycatalytic CBHI complexes in this study. CBHI/MNP-PAA and CBHI/MNP-PMAA were made by conjugating CBHI on MNP-PAA and MNP-PMAA, respectively, and magnetically separated from unbound CBHI. The

system is, thus free of interference from individual freely dispersed enzymes, either before or after their adsorption on the cellulose. We chose Avicel which is a microcrystalline cellulose with 60-80% crystallinity as the targeted substrate.[39] Upon mixing CBHI-MNP complexes with Avicel, the complexes adsorbed on the surface of Avicel and facilitated the magnetic separation of Avicel particles (**Figure 3.6A**) as the complexes are strongly adhered to Avicel surface. The distribution of the complexes on the surface of Avicel is shown in the field emission scanning electron microscopy (FESEM) (**Figure 3.6B**).

A

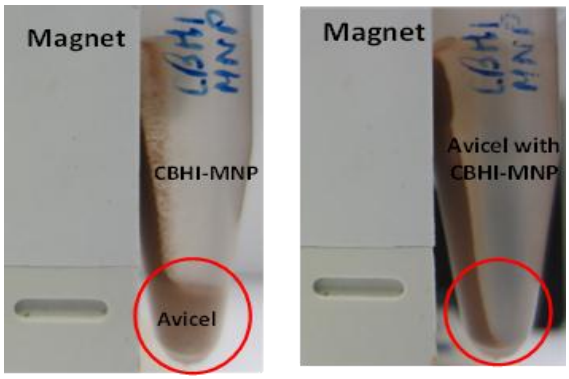

B

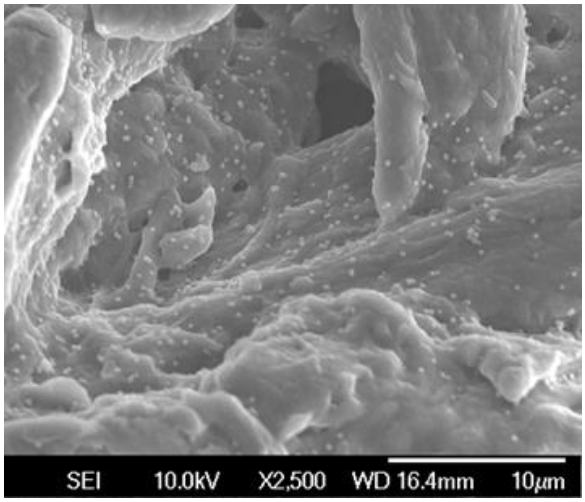

Figure 3.6: Adsorption of polycatalytic cellulase complexes on Avicel cellulose. (**A**) The response of Avicel cellulose to magnet before (left panel) and after (right panel) incubation with

CBHI/MNP-PAA for 2 hr. (**B**) FESEM image of CBHI/MNP-PAA (bright dots in the image) on Avicel. Samples were incubated with CBHI/MNP-PAA for 6 hrs and washed 5 times with Tris-HCl buffer.

The kinetics of adsorption to Avicel and subsequent hydrolytic reactions to release soluble sugar (cellobiose and glucose) were followed at 37 ˚C using different initial concentrations of CBHI/MNP-PAA, CBHI/MNP-PMAA and CBHI, and enzyme-to-substrate ratios. The time courses of adsorption as a fraction of total enzyme and the amount of soluble sugars released was presented in **Figure 3.7**. The attachment of CBHI onto polycatalytic complexes changed both adsorption and activity, relative to those of CBHI. Compared to the rate of adsorption of CBHI, the binding of CBHI/MNP-PAA and CBHI/MNP-PMAA to Avicel was slower, required more than 2 hours to reach saturation. The process depended on the concentrations of enzyme and Avicel (**Figure 3.7A-C**). At the same Avicel concentration, the adsorption of CBHI complexes is lower than adsorption of CBHI. Increasing the Avicel concentration enhanced the adsorption (**Figure 3.7C**) up to 85% adsorption reached at an Avicel concentration of 60 mg/ml (or ~6 wt%). In all cases, the overall adsorption was not affected as hydrolysis of Avicel proceeded.

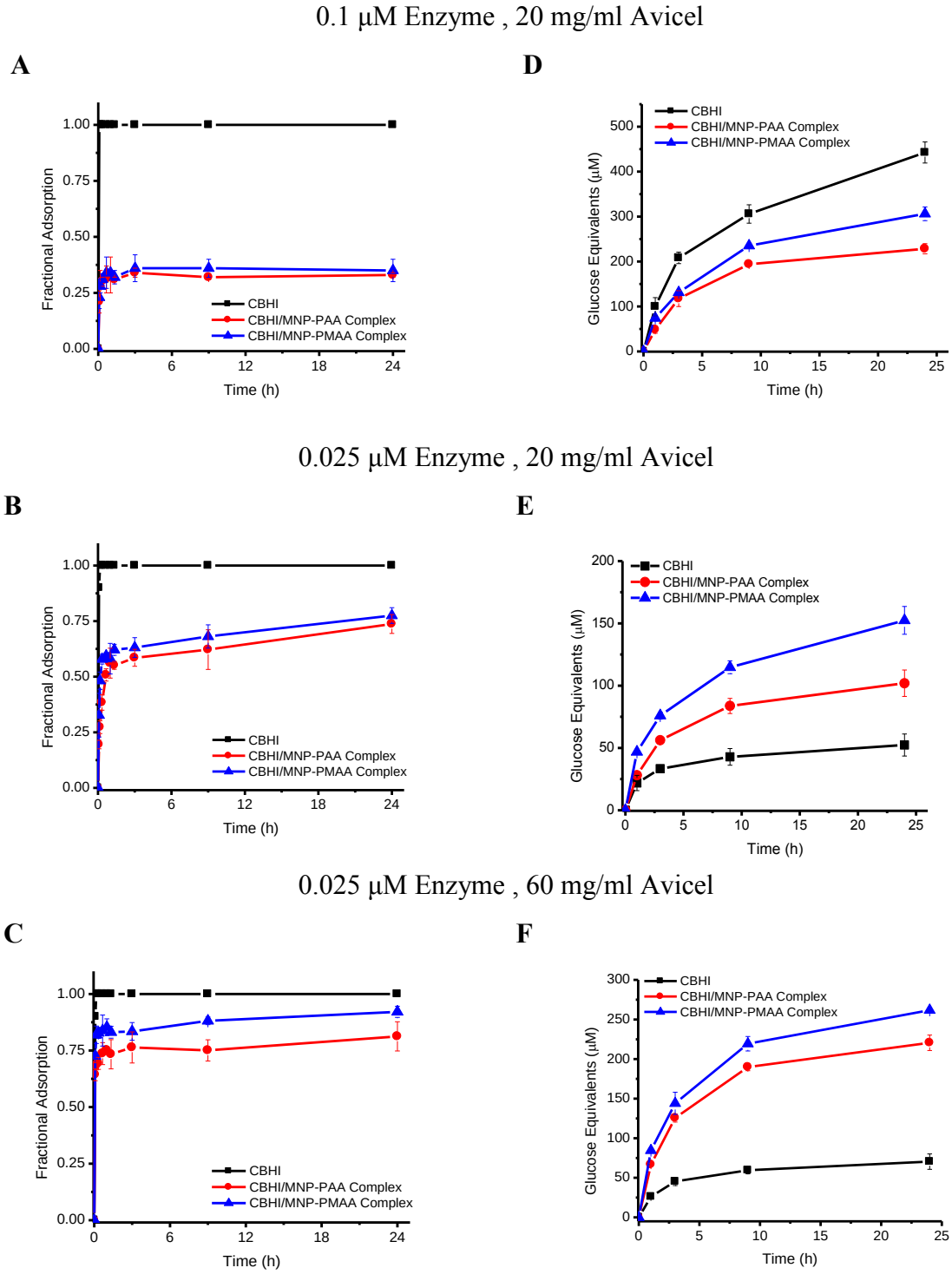

Figure 3.7: Adsorption kinetics (A-C) and hydrolysis kinetics (D-F) of Avicel by CBHI in the free state (as black square), CBHI/MNP-PAA complex (as red circle) and CBHI/MNP-PMAA

complex (as blue triangle). Initial concentrations of total enzymes and Avicel are as indicated. Incubation was at 37 ºC in 5 mM Tris-HCl, pH 6.5. At the given times, Avicel was separated from the enzyme complexes or the free enzyme by sedimentation. The supernatant was used to determine concentrations of unbound complexes/enzymes and soluble sugar.

3.3.3 Analysis of the Adsorption Isotherms. The adsorption isotherms with 20 mg/ml Avicel at 37 ˚C is shown in **Figure 3.8**. The complex concentrations in Figure 3.4.A were determined by dividing the molarity of complexed CBHI with the estimated number of CBHI per particle. Due to the heterogeneous nature of Avicel surface and different binding characteristics of free and non-complexed CBHI, Langmuir-Freundlich (LF) model was used to analyze the adsorption isotherms.[40] LF isotherm is able to model the adsorption behavior of both homogeneous and heterogeneous systems, and suitable for the comparisons of adsorption with very different underlying mechanisms. The binding parameters can be determined directly using the LF fitting coefficients that yield a measure of the total number of binding sites, mean binding affinity and heterogeneity. [40] The equation for the LF model is as follows:

$$B = \frac{N_t a F^m}{1 + a F^m} \qquad (1)$$

where B and F are equilibrium concentration of bound and unbounded enzymes or enzyme complexes. N_t is the maximum binding capacity, m is the heterogeneity index, which varies from 0 to 1 (e.g., $m = 1$ for a homogeneous material and for $m < 1$ for heterogeneous material). The variable a is related to the mean binding affinity (K_A) as $K_A = a^{1/m}$. Based on the LF model, the mean binding affinity, the maximal binding capacities, and the heterogeneity index

(equivalent to the inverse of the cooperativity factor in a Hill equation) were derived from the adsorption isotherms (**Table 3.1**).

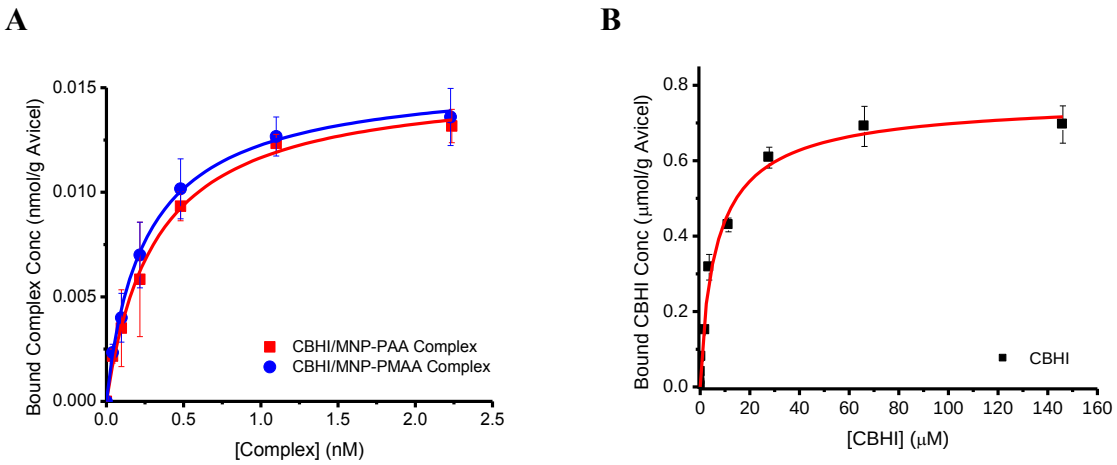

Figure 3.8: Adsorption of polycatalytic cellulase complexes on Avicel cellulose. Adsorption isotherms of (A) CBHI/MNP-PAA complex, CBHI/MNP-PMAA complex, and (B) CBHI on Avicel. Avicel concentration was kept constant (20 mg/ml), at increasing enzyme concentrations.

Table 3.1. Mean binding affinity, binding capacities and the heterogeneity index for the adsorption of the polycatalytic complexes and the CBHI to Avicel.

Sample	[a]Mean Binding Affinity (M^{-1})	[b]Binding Capacity (µmol enzyme / g Avicel)	Heterogeneity Index
CBHI/MNP-PAA	$(3.1 \pm 0.6) \times 10^9$	0.0046 ± 0.0004	0.99 ± 0.11
CBHI/MNP-PMAA	$(4.1 \pm 0.4) \times 10^9$	0.0045 ± 0.0001	1.02 ± 0.06
CBHI	$(1.4 \pm 0.3) \times 10^5$	0.77 ± 0.04	0.86 ± 0.09

[a] The binding affinity of CBHI/MNP-PAA or CBHI/MNP-PMAA is expressed on the basis of the concentration of particles.

[b] To compare with CBHI, the binding capacity for the CBHI/MNP-PAA or CBHI/MNP-PMAA is expressed on the basis of the number of CBHI enzyme molecules.

Table 3.1 shows that the binding affinities of CBHI/MNP-PAA and CBHI/MNP-PMAA are several orders of magnitude higher than that of CBHI. Such tight binding indicates that the polycatalytic complex is bound to Avicel through multivalent interactions, and almost irreversible in practice. The maximal binding capacity for CBHI/MNP-PAA and CBHI/MNP-PMAA is similar, but about 160 times lower than that of CBHI. Normally, high surface binding capacity will require some rearrangement of the molecules that are already bound to the surface,[41] in order to optimize the distribution of molecules for higher coverage. The simultaneous low binding capacity and high apparent affinity found for the CBHI complexes suggest the lack of mobility of the complexes on Avicel, or the existence of strong negative cooperativity in the binding process (e.g., through electrostatic repulsion from the net charges of large complexes). The heterogeneity index obtained from fitting the binding isothermals to LF model is found to less than 1 for the CBHI, as expected from the heterogeneous nature of Avicel surface, which contains different types of binding sites.[6] In contrast, the heterogeneity indexes for both CBHI complexes were found to be around 1. Unlike CBHI, these large complexes cannot distinguish the heterogeneous nature of the Avicel surface, as the binding is the collective behavior of a large number of CBHI enzymes in the complex.

3.3.4 Hydrolytic Efficiency of Polycatalytic CBHI Complexes on Cellulose. **Figure 3.7D-F** compares the apparent hydrolytic efficiency of CBHI complexes and CBHI on Avicel, by measuring the amount of soluble sugars (e.g., as glucose equivalents) released from Avicel at an identical total enzyme concentration. **Figure 3.7D** shows that, at higher enzyme-to-cellulose

ratio, CBHI have better hydrolytic efficiency than the polycatalytic CBHI complexes. But at the lower enzyme-to-cellulose ratios (**Figure 3.7E, F**), both CBHI/MNP-PAA and CBHI/MNP-PMAA exhibited significantly greater efficiency compared to the CBHI. **Figure 3.7F** shows that the soluble sugars released in 24 hrs, increased by 500% in the case of CBHI/MNP-PMAA at 6% (w/v) of Avicel, when compared to the product produced at the same concentration of CBHI. The adsorption levels of CBHI complexes strongly depend on the concentration of enzymes and cellulose, due to their low binding capacity (**Figure 3.7A-C** and **Figure 3.3.9**). In contrast, almost 100% of the CBHI adsorbed on the cellulose surface in the three different enzyme-to-cellulose ratios examined. The control experiments on the MNP-PAA and MNP-PMAA without enzymes show that the colloidal scaffolds alone do not have hydrolytic activity in degrading cellulose.

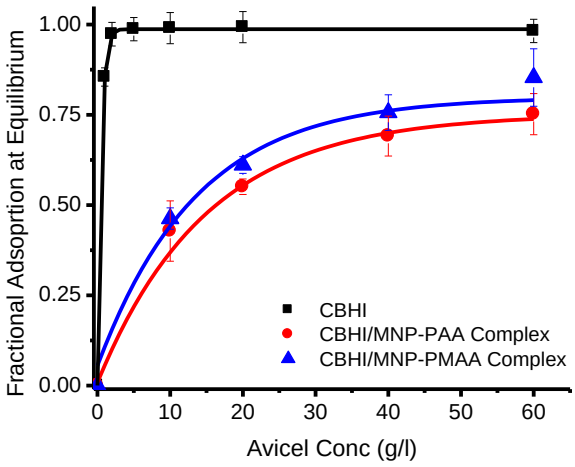

Figure 3.9 : Effect of Avicel concentration on the adsorption of CBHI/MNP-PAA, CBHI/MNP-PMAA and free CBHI. The total enzyme concentration was kept constant at 0.025 μM, while successively higher concentrations of Avicel were applied.

To compare the inherent hydrolytic activity between CBHI and CBHI-MNP complexes, we calculated the reaction productivity by normalizing the amount of released soluble sugar after 24 hrs, according to the actual fraction of enzyme complexes or enzymes bound on the cellulose. **Figure 3.10** shows that, after correction, both the CBHI/MNP-PAA and CBHI/MNP-PMAA have significantly higher productivity than the CBHI at these enzyme concentrations, but the gap gradually decreases with increasing enzyme concentration. The extent of activity enhancement found with the complexes is remarkable, but somewhat puzzling. Individual CBHI molecules are known to rely on processive motion on the track of the crystalline cellulose to carry out the hydrolytic reactions continuously and release the cellobiose.[31,42,43] Very unlikely, the large number of CBHI molecules on MNP-PAA or MNP-PMAA can coordinate their motions collectively to facilitate a similar, processive motion as a whole unit. Then, what are the possible mechanisms that facilitate the remarkable hydrolytic efficiency of CBHI complexes?

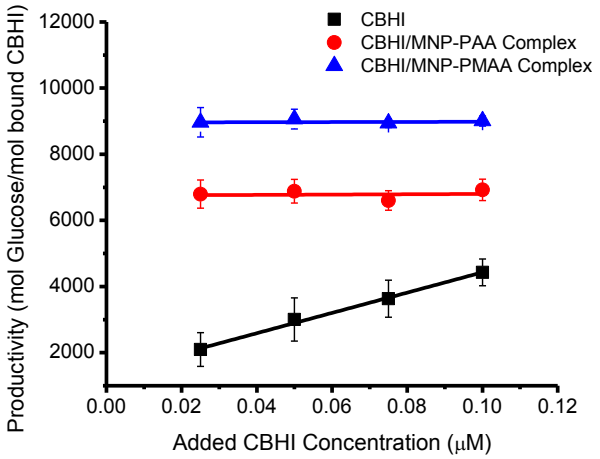

Figure 3.10: The effect of total enzyme concentration on the reaction productivities of CBHI complexes and CBHI. Amount of soluble sugar released was measured from the solutions after incubating CBHI or CBHI complexes with 20 mg/ml Avicel for 24 hr at 37ºC in 5 mM Tris-HCl

buffer, pH 6.5. Productivity was determined by normalizing the amount of soluble sugars released with the amount of enzymes bound on the cellulose substrate.

Careful examination of the adsorption and the hydrolysis kinetics (**Figure 3.7**) indicates that the hydrolytic reactions of the CBHI almost ceased within five hours at the low enzyme concentrations, suggesting that at these conditions, most adsorbed CBHI were trapped on the obstacles on the heterogeneous cellulose surface and lost their processive motions (i.e., processivity) at the late stage. [44] The so-called "jamming" of CBHI on crystalline cellulose is a known phenomenon, as found in a recent study using high-speed atomic force microscopy (HS-AFM).[45] The dissociation rate constants (k_{off}) for CBHI were previously reported with values in the range of 10^{-3} s^{-1}, corresponding to a half-life on Avicel around 10 mins.[44] Therefore, regaining the processivity of jammed CBHI through the way of desorption and re-adsorption is relatively ineffective. Instead, accumulation of multiple CBHI molecules behind the blocked one leads to the elimination of the obstacle, and the coordinated action of the "on-site" clusters may be an effective mechanism to regain processivity of trapped CBHI: a cooperative behavior.[45] The probability of forming such clusters on the trapped sites depends on the concentration of mobile enzymes bound on the surface of cellulose. Therefore, by adding more CBHI to the system will favor the temporal aggregation of multiple enzymes on the obstacle sites and facilitate the elimination of the obstacles for processive motion. This hypothesis seems to be supported by examining the hydrolytic reactions of Avicel by CBHI at higher concentrations (e.g., 0.5 μM), which shows the continuity of the reaction even after 24 hrs, and the doubling of productivity of CBHI when the enzyme concentration increases from 0.1 μM to 0.5 μM (**Figure 3.11**).

A B

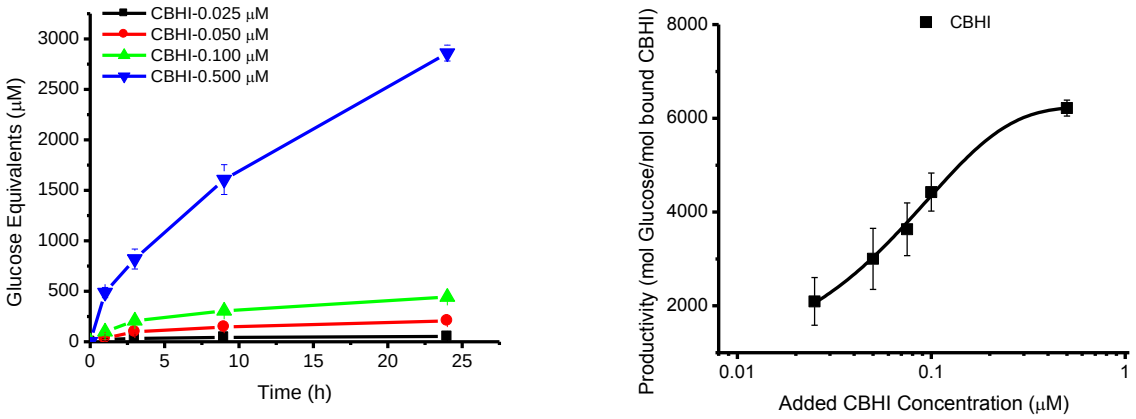

Figure 3.11: (**A**) Hydrolytic activity of free CBHI with increasing concentrations. (**B**) Comparison of the average productivities of CBHI at different concentrations. Avicel concentration was kept constant at 20 mg/ml. The reactions were carried out at 37°C in 5 mM Tris-HCl buffer at pH 6.5. Enzyme productivities were measured by normalizing amount of glucose equivalents released in 24 hr by the amount of cellulose bound enzymes.

In contrast, the hydrolytic reactions of Avicel by polycatalytic CBHI complexes follow a different pattern from the CBHI (**Figure 3.10**). Even at very low enzyme concentrations, activities of bound complexes remain high. Increasing the enzyme concentration contributes insignificantly to the productivity of the bound complexes (**Figure 3.10**). And **Figure 3.7D-F** shows that, in all experiments, the activity of the bound complexes did not prevail with time (slowed down substantially in less than ten hours). Apparently, the short-range processive motion of individual CBHI tethered to the flexible PMAA or PAA scaffolds are allowed, judging from the high productivity of the complexes. But the complex may not have the processive motion or long-range mobility as a collective unit. For polycatalytic complexes, the effective concentration of CBHI in contact with cellulose largely depends on the grafting densities of enzymes in the complex rather than the bulk concentration of enzymes. The high local molarity

of enzymes in our complexes seems to facilitate some cooperative behaviors similar to that found in the temporal clustering of the free enzymes in overcoming the obstacles. Consequently, at low total enzyme concentrations especially, CBHI complexes have significant advantages relative to CBHI. The physical property of the supporting scaffolds also has the effect on the cooperative behaviors of the tethered enzymes. PMAA, which is more rigid than PAA, appears to be a better choice for the scaffold materials. However, the large polycatalytic complex lack long-range surface mobility, and their extremely tight, polyvalent nature of the binding to the cellulose precludes desorption as an effective, alternative way to relocate the complexes on new substrate sites. Therefore, when the concentration of bound enzyme was increased to a level comparable to the local molarity of enzymes in the complexes, CBHI eventually becomes more effective (**Figure 3.11**) by taking advantage of both the agility of individual processive motions and the cooperative mechanism in overcoming the obstacle sites to regain processivity.

3.3.5 Effect of Enzyme Grafting Densities and Particle Sizes on the Surface Adsorption and Hydrolytic Activities of the Polycatalytic CBHI complexes on Cellulose. Based on the proposed mechanism, the high local molarity of enzymes in the complexes plays an important role in enhancing the effectiveness of enzyme complexes at low total enzyme concentrations. We prepared two additional CBHI/MNP-PAA samples that have the same colloidal core but possess different grafting densities of CBHI on the surface (around 150 and 400 enzymes per complex), and compared their hydrolytic activities at the same total enzyme concentrations. **Figure 3.12** shows how the hydrolytic activities of the CBHI complexes depended on the grafting densities of enzymes. Increasing the local concentration of enzymes in the complexes clearly enhances the activities of the polycatalytic complexes, but the maximum grafting density is limited by the conjugation method used and specific enzyme interactions. We also examined the CBHI

complexes that have identical surface density of enzymes but have different core sizes. As expected, the complexes with smaller cores have larger binding capacity to Avicel (**Figure 3.13**), presumably due to their smaller footprint. After correcting for their adsorption levels, the specific activities of different-sized complexes do not vary much (**Figure 3.13**), indicating that the inherent reactivity of the polycatalytic complexes is mainly determined by the local organization of enzymes.

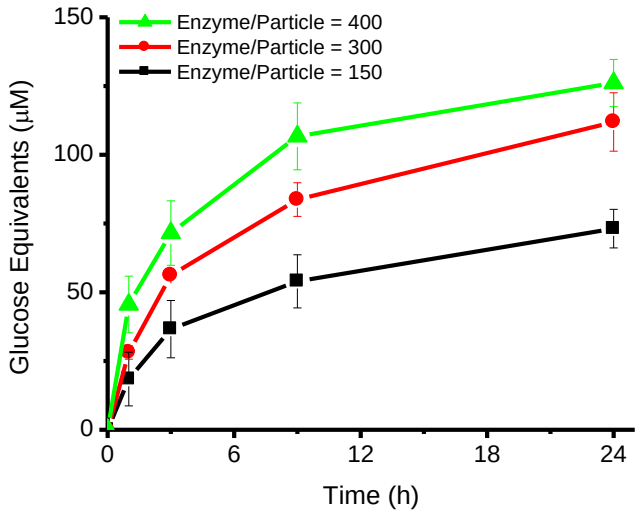

Figure 3.12: Effect of grafting density on the hydrolysis of CBHI/MNP-PAA complex. The total enzyme concentration and Avicel concentration were kept constant at 0.025μM and 20mg/ml, respectively, and incubation was at 37ºC in 5mM Tris-HCl, pH 6.5. At the given times, the Avicel was separated from the enzyme complexes by sedimentation.

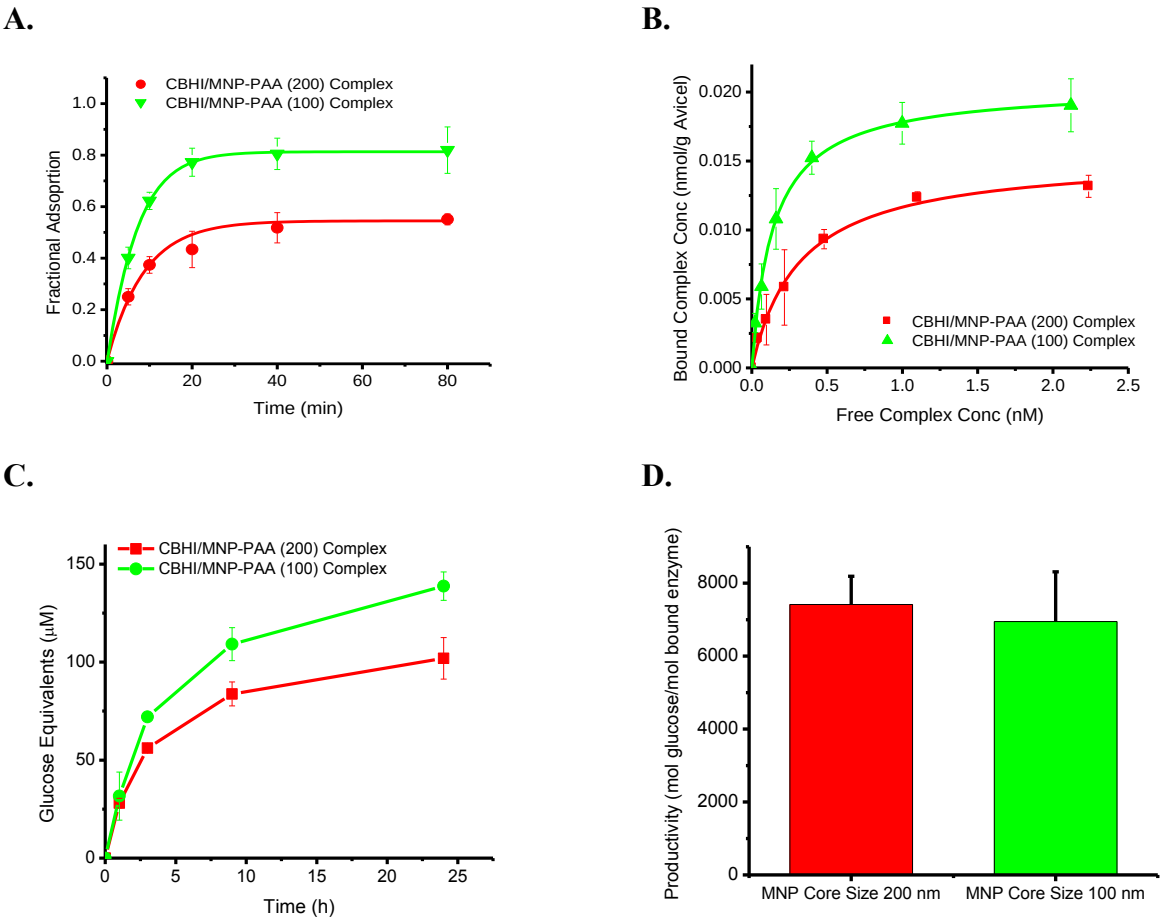

Figure 3.13: Effect of particle sizes on the adsorption and hydrolysis kinetics of CBHI/MNP-PAA complex. (**A**) Comparison of the time-dependent adsorption of CBHI/MNP-PAA complexes with two different MNP core sizes. (**B**) Comparison of the adsorption isotherm of CBHI/MNP-PAA complexes with two different MNP core sizes. (**C**) Comparison of the hydrolysis kinetics of CBHI/MNP-PAA complexes with two different MNP core sizes. (**D**) Comparison of the average productivity of CBHI/MNP-PAA complexes with two different MNP core sizes. In all the experiments here, the total enzyme concentration and Avicel concentration were kept constant at 0.025 μM and 20 mg/ml, respectively. Enzyme productivities were measured by normalizing amount of glucose equivalents released in 24 hr by the amount of cellulose bound enzymes.

3.3.6 Trace the Motion of Individual CBHI Complexes on Cellulose Film using Total Internal Reflection Fluorescence Microscopy (TIRFM). We used TIRFM to examine the adsorption/desorption and surface mobility of individual CBHI complexes on cellulose thin films, to confirm our findings derived from the experiments based on ensemble behavior. Avicel was first dissolved in ionic liquids and the diluted solution was spun cast onto microscope cover-slide and annealed under controlled environment to prepare a smooth film of regenerated cellulose with a thickness of ~50 nm and crystallinity of ~80%. CBHI/MNP-PAA complexes were conjugated with fluorescein isothiocyanate (FITC) for fluorescence imaging, and introduced into the buffer solution above the cellulose thin film. Under TIRFM, only the particles bound on the cellulose thin film (within ~100 nm distance from the cover slide) are visible. Therefore, the adsorption and desorption of individual CBHI complexes on cellulose film can be readily followed using time-lapse TIRFM imaging, and their surface motions can be individually traced with great accuracy. **Figure 3.14** shows a set of representative data on the adsorption of CBHI/MNP-PAA onto regenerated cellulose thin film (see the supplemental materials for the movie that has been sped up 50 times). Once bounded, the complexes rarely desorbed from the cellulose surface in the time scale of the experiments (~1 hr), in agreement with the apparent dissociation constants measured. The time-dependent positions of individual complexes were analyzed, based on a particle-tracing program (CISMM Video Spot Tracker, http://www.cismm.org/downloads/), and corrected for the stage drifting (~3 nm/s). **Figure 3.15** shows the individual traces of 20 complexes after they bound on the cellulose film. Unlike the processive CBHI which moves as fast as 5 nm/s on the cellulose,[45] the CBHI complex as a whole unit, is incapable of moving any large, detectable distance in our experiments. This supports our

proposed mechanism in explaining the different hydrolytic reactivity found in the enzyme complexes.

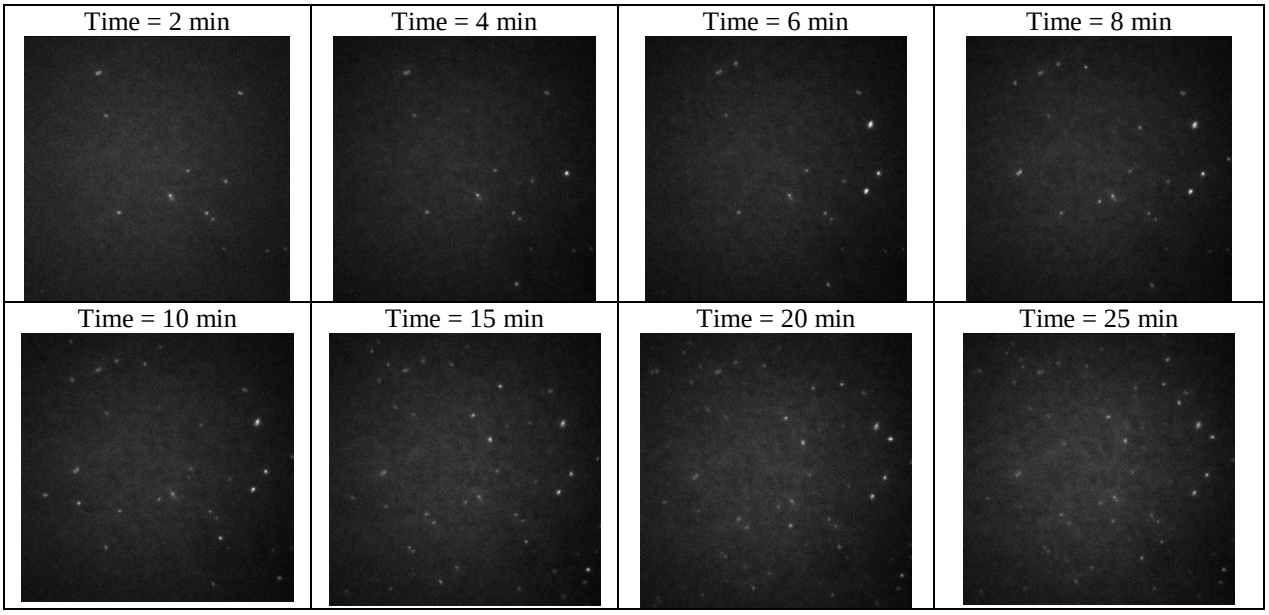

Figure 3.14. Time-dependent TIRF study on the adsorption and motion of CBHI/MNP-PMAA Complexes on the cellulose thin film. The experiment was performed in 5 mM Tris HCl buffer at 37°C. The images have a size of 87 μm × 87 μm.

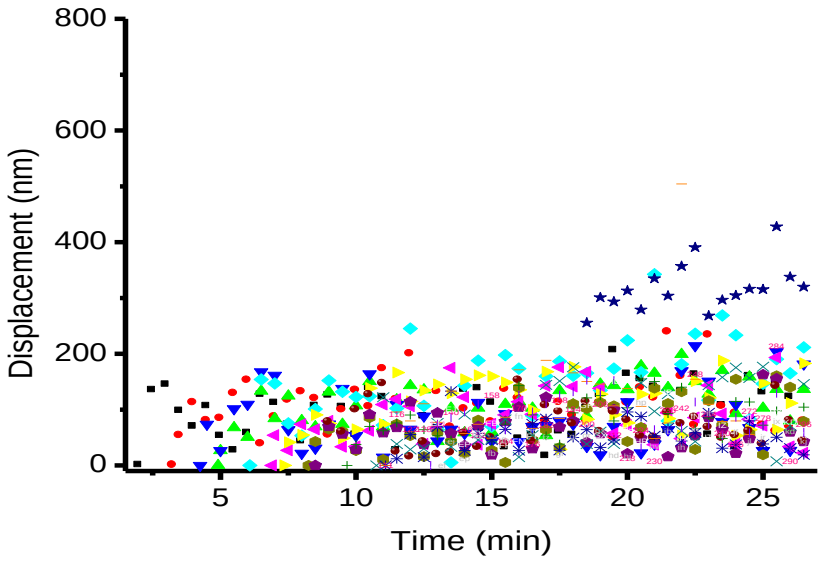

Figure 3.15: Displacement of individual CBHI/MNP-PMAA complexes from the original adsorption sites on the cellulose thin film.

3.4 CONCLUSIONS

The formation of polycatalytic clusters of cellulases on colloidal polymers increase the rate of hydrolytic reactions on cellulose, but mainly at relatively low cellulase-to-cellulose ratios. At these conditions, the free enzymes are prone to get "jammed" at the obstacles on the cellulose surface. The polycatalytic complexes, on the other hand, facilitate effective polyvalent contacts between a high local molarity of enzymes and cellulose, for enhanced efficiency in the hydrolytic reactions. However, once bound, the polycatalytic complexes can only carry out reactions locally and not capable of relocating to new sites due to their lack of long-range surface mobility and their extremely tight binding. Therefore, at increased cellulase-to-cellulose ratios, free enzymes gradually become more effective due to their much higher binding capacity and presumably with the help of a cooperative mechanism that regains the processivity of trapped

enzyme by the formation of clusters on-site to clear the barriers. The opportunity in the development of highly optimized polycatalytic complexes across different concentration ranges may come from the design of new nano-scaffolds that can indeed coordinate the motions of individual enzymes in the complex, and that can couple the external forces to gain motility to speed up the overall enzymatic reactions.

REFERENCES

1. Hill, J.; Nelson, E.; Tilman, D.; Polasky, S.; Tiffany, D. *Proceedings of the National Academy of Sciences of the United States of America* **2006**, *103*, 11206.
2. Himmel, M. E.; Ding, S.-Y.; Johnson, D. K.; Adney, W. S.; Nimlos, M. R.; Brady, J. W.; Foust, T. D. *Science (Washington, DC, U. S.)* **2007**, *315*, 804.
3. Ding, S.-Y.; Liu, Y.-S.; Zeng, Y.; Himmel, M. E.; Baker, J. O.; Bayer, E. A. *Science (Washington, DC, U. S.)* **2012**, *338*, 1055.
4 Chang, M. C. Y. *Current Opinion in Chemical Biology* **2007**, *11*, 677.
5. Doi, R. H.; Kosugi, A. *Nature Reviews Microbiology* **2004**, *2*, 541.
6. Staahlberg, J.; Johansson, G.; Pettersson, G. *Bio/Technology* **1991**, *9*, 286.
7. Nidetzky, B.; Claeyssens, M.; Steiner, W. *Biotechnol. Pulp Pap. Ind., Proc* **1996**, 537.
8. Jalak, J.; Kurasin, M.; Teugjas, H.; Vaeljamaee, P. *Journal of Biological Chemistry* **2012**, *287*, 28802.
9. Bayer, E. A.; Lamed, R. *J. Bacteriol.* **1986**, *167*, 828.
10. Fierobe, H.-P.; Bayer, E. A.; Tardif, C.; Czjzek, M.; Mechaly, A.; Belaich, A.; Lamed, R.; Shoham, Y.; Belaich, J.-P. *Journal of Biological Chemistry* **2002**, *277*, 49621.
11. Ding, S. Y.; Xu, Q.; Crowley, M.; Zeng, Y.; Nimlos, M.; Lamed, R.; Bayer, E. A.; Himmel, M. E. *Current Opinion in Biotechnology* **2008**, *19*, 218.
12. Bayer, E. A.; Belaich, J. P.; Shoham, Y.; Lamed, R. *Annual Review of Microbiology* **2004**, *58*, 521.
13. Fierobe, H.-P.; Bayer Edward, A.; Tardif, C.; Czjzek, M.; Mechaly, A.; Belaich, A.; Lamed, R.; Shoham, Y.; Belaich, J.-P. *J Biol Chem* **2002**, *277*, 49621.

14. Fierobe, H.-P.; Mingardon, F.; Mechaly, A.; Belaich, A.; Rincon, M. T.; Pages, S.; Lamed, R.; Tardif, C.; Belaich, J.-P.; Bayer, E. A. *Journal of Biological Chemistry* **2005**, *280*, 16325.

15. Hammel, M.; Fierobe, H.-P.; Czjzek, M.; Kurkal, V.; Smith, J. C.; Bayer, E. A.; Finet, S.; Receveur-Brechot, V. *Journal of Biological Chemistry* **2005**, *280*, 38562.

16. Tebeka, I. R. M.; Silva, A. G. L.; Petri, D. F. S. *Langmuir* **2009**, *25*, 1582.

17. Ho, K. M.; Mao, X.; Gu, L.; Li, P. *Langmuir* **2008**, *24*, 11036.

18. Kim, D.-M.; Umetsu, M.; Takai, K.; Matsuyama, T.; Ishida, N.; Takahashi, H.; Asano, R.; Kumagai, I. *Small* **2011**, *7*, 656.

19. Hirsh, S. L.; Bilek, M. M. M.; Nosworthy, N. J.; Kondyurin, A.; dos Remedios, C. G.; McKenzie, D. R. *Langmuir* **2010**, *26*, 14380.

20. Cho, E. J.; Jung, S.; Kim, H. J.; Lee, Y. G.; Nam, K. C.; Lee, H.-J.; Bae, H.-J. *Chem. Commun. (Cambridge, U. K.)* **2012**, *48*, 886.

21. Blanchette, C.; Lacayo, C. I.; Fischer, N. O.; Hwang, M.; Thelen, M. P. *PLoS One* **2012**, *7*, e42116.

22. MacKenzie, K. J.; Francis, M. B. *J Am Chem Soc* **2012**, *135*, 293.

23. Liao, H.; Chen, D.; Yuan, L.; Zheng, M.; Zhu, Y.; Liu, X. *Carbohydr. Polym.* **2010**, *82*, 600.

24. Nidetzky, B.; Steiner, W.; Claeyssens, M. *Biochem J* **1994**, *303 (Pt 3)*, 817.

25. Boraston, A. B.; Bolam, D. N.; Gilbert, H. J.; Davies, G. J. *Biochem. J.* **2004**, *382*, 769.

26. Poon, D. K. Y.; Withers, S. G.; McIntosh, L. P. *Journal of Biological Chemistry* **2007**, *282*, 2091.

27. Nidetzky, B.; Steiner, W.; Hayn, M.; Claeyssens, M. *Biochemical Journal* **1994**, *298*, 705.

28. Beckham, G. T.; Bomble, Y. J.; Matthews, J. F.; Taylor, C. B.; Resch, M. G.; Yarbrough, J. M.; Decker, S. R.; Bu, L. T.; Zhao, X. C.; McCabe, C.; Wohlert, J.; Bergenstrahle, M.; Brady, J. W.; Adney, W. S.; Himmel, M. E.; Crowley, M. F. *Biophys. J.* **2010**, *99*, 3773.

29. Divne, C.; Stahlberg, J.; Teeri, T. T.; Jones, T. A. *Journal of Molecular Biology* **1998**, *275*, 309.

30. Ting, C. L.; Makarov, D. E.; Wang, Z. G. *J. Phys. Chem. B* **2009**, *113*, 4970.

31. Igarashi, K.; Koivula, A.; Wada, M.; Kimura, S.; Penttilae, M.; Samejima, M. *Journal of Biological Chemistry* **2009**, *284*, 36186.

32. Igarashi, K.; Koivula, A.; Wada, M.; Kimura, S.; Penttila, M.; Samejima, M. *Journal of Biological Chemistry* **2009**, *284*, 36186.

33. Ma, W.; Xu, S.; Li, J.; Guo, J.; Lin, Y.; Wang, C. *J. Polym. Sci., Part A: Polym. Chem.* **2011**, *49*, 2725.

34. Zhang, Y.; Yang, Y.; Ma, W.; Guo, J.; Lin, Y.; Wang, C. *ACS Appl. Mater. Interfaces* **2013**, *5*, 2626.

35. Staros, J. V.; Wright, R. W.; Swingle, D. M. *Anal. Biochem.* **1986**, *156*, 220.

36. Heptinstall, J.; Stewart, J. C.; Seras, M. *Enzyme Microb. Technol.* **1986**, *8*, 70.

37. Liu, Y.-S.; Baker, J. O.; Zeng, Y.; Himmel, M. E.; Haas, T.; Ding, S.-Y. *Journal of Biological Chemistry* **2011**, *286*, 11195.

38. Chanzy, H.; Henrissat, B.; Vuong, R.; Schulein, M. *FEBS Letters* **1983**, *153*, 113.

39. Hall, M.; Bansal, P.; Lee, J. H.; Realff, M. J.; Bommarius, A. S. *Febs J.* **2010**, *277*, 1571.

40. Umpleby, R. J., II; Baxter, S. C.; Chen, Y.; Shah, R. N.; Shimizu, K. D. *Anal. Chem.* **2001**, *73*, 4584.

41. Sugimoto, N.; Igarashi, K.; Wada, M.; Samejima, M. *Langmuir* **2012**, *28*, 14323.

42. Fox, J. M.; Levine, S. E.; Clark, D. S.; Blanch, H. W. *Biochemistry* **2011**, *51*, 442.

43. Bu, L. T.; Nimlos, M. R.; Shirts, M. R.; Stahlberg, J.; Himmel, M. E.; Crowley, M. F.; Beckham, G. T. *Journal of Biological Chemistry* **2012**, *287*, 24807.

44. Kurasin, M.; Vaeljamaee, P. *Journal of Biological Chemistry* **2011**, *286*, 169.

45. Igarashi, K.; Uchihashi, T.; Koivula, A.; Wada, M.; Kimura, S.; Okamoto, T.; Penttilae, M.; Ando, T.; Samejima, M. *Science (Washington, DC, U. S.)* **2011**, *333*, 1279.

46. Medve, J.; Lee, D.; Tjerneld, F. *J. Chromatogr., A* **1998**, *808*, 153.

47. Huggett, A. S.; Nixon, D. A. *Lancet* **1957**, *273*, 368.

48. Swatloski, R. P.; Spear, S. K.; Holbrey, J. D.; Rogers, R. D. *J Am Chem Soc* **2002**, *124*, 4974.

49. Cao, Y.; Li, H.; Zhang, Y.; Zhang, J.; He, J. *J. Appl. Polym. Sci.* **2010**, *116*, 547.

Chapter 4

Polycatalytic Nanocomplex with Non-processive Cellulases Immobilized on the Surface

ABSRACT : Formation of polycatalytic cellulase complexes significantly enhances the substrate binding in the integrated supramolecular structure, and the prospect of having consistent, multiple attacks on cellulose chains improves its inherent productivity. However, the overall performance of polycatalytic complexes is limited by the accessibility and mobility of complexes on the cellulose substrate.

4.1 INTRODUCTION

Enzymatic hydrolysis of cellulose is an important process involved in the conversion of biomass into biofuels under mild conditions, and the modification of the cellulosic materials for desired properties.[1] Although the chemical composition of cellulose is simple, the structure and morphology of native cellulose are complex and not uniform, containing both crystalline and amorphous regions. Efficient hydrolysis of cellulose requires the cooperative actions of at least three types of enzymes: exoglucanases (also called cellobiohydrolases), endoglucanases and β-glucosidase.[2] Exoglucanases such as CBHI produced by the filamentous fungus *Trichoderma reesei* are processive enzymes, which bind to the ends of the cellulose chains in crystalline regions and "slide" along the chains progressively for continuing reactions.[3] Cellobiose and glucose are released as the reaction products from the processive motions of exoglucanases. In contrast, endoglucanase such as EGII of *T. reesei* are thought to be non-processive, and preferably

attack more disordered regions of cellulose by cleaving the bonds in the middle of chains. Interestingly, significant amounts of cellobiose and glucose were still found in the hydrolysis of microcrystalline cellulose (e.g., Avicel) by EGII, and the proportion of the soluble sugar products also varied considerably with the enzyme-to-substrate ratio and the reaction time. As the soluble sugars are not the expected products of a typical endoglucanase activity on a solid substrate, the sugar production pattern of EGII suggested that either multiple random attacks can happen on individual cellulose chains resulting in small fragments that can be further hydrolysed in solution, or two-domain endoglucanases may possess some "pseudo-processivity" from their cellulose binding domain (CBD).

We are interested in understanding whether the formation of artificial polycatalytic complexes from endoglucanase will further improve their capability in producing soluble sugars, as a consequence of improved substrate binding and the proximity of multiple enzymes that may act on cellulose substrate in a concerted manner. Polycatalytic cellulase complexes made by immobilization of industrial cellulases on polymer or nanoparticle scaffolds are technologically attractive due to the low-cost and recyclability of these synthetic nanoscaffolds, and the scale-up potential for biorefinery applications.[4-6] However, the relatively large, polycatalytic complexes could possess quite different adsorption behaviour and hydrolytic activity on cellulose, in relative to the corresponding cellulases in their free state (**Figure 4.1**). First, the specific area of cellulose for binding and reactions may decrease considerably as most of the internal surface area of porous cellulose is not be accessible to large complexes. Second, once bound, the cellulase complexes may tend to stay on the surface of cellulose as a consequence of polyvalent

contacts between a high local molarity of enzymes and the cellulose substrate. Third, distinct reaction activities or product patterns may be observed in the complexes due to the proximity of enzymes and their collective actions. It is thus crucial to understand the benefit and limit of the approach before polycatalytic complexes from industrial cellulases can be rationally designed to achieve maximal hydrolytic efficiency.

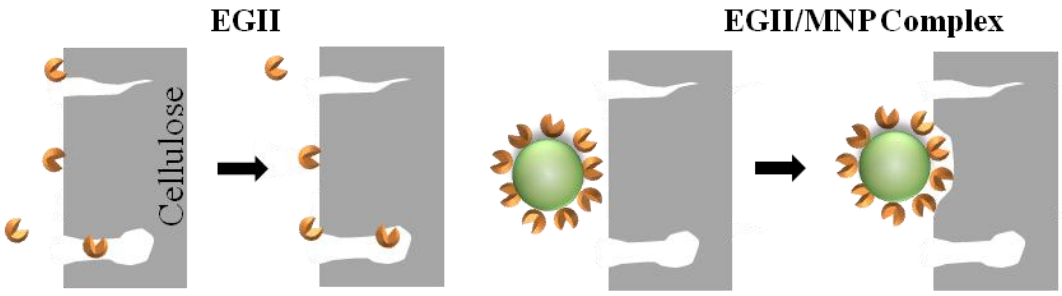

Figure 4.1: Schematic of the adsorption and reaction of polycatalytic endoglucanase complexes on the surface of microcrystalline cellulose.

Herein, we synthesized polycatalytic complexes by the immobilization of EGII on the surface of colloidal polymers with a magnetic nanoparticle (MNP) core, and compared their adsorption to Avicel cellulose and their activities in the production of soluble sugars to EGII in its free state. The study shows that the formation of polycatalytic complexes significantly enhances the substrate binding in the integrated supramolecular structure, and the prospect of having consistent, multiple attacks on cellulose chains to produce soluble sugars. The overall performance of polycatalytic complexes, however, is limited by the accessibility of complexes on the cellulose substrate.

4.2 EXPERIMENTAL

4.2.1 Materials. Cellulase mixture from *Trichoderma reesei* (Celluclast® 1.5 L from Novozymes), β-glucosidase (Novozymes 188), glucose oxidase, horseradish peroxidase, papain, microcrystalline cellulose (Avicel, PH101) and 4-methylumbelliferyl β-D-cellobioside were purchased from Sigma-Aldrich. All other chemicals were of analytical grade and purchased from Fisher Scientific. EGII was purified from cellulase mixture as described,[46] using GE FPLC equipped with ion exchange columns. The purity of EGII and other individual enzymes were verified by their molecular weights using SDS-PAGE, MS and by the very sensitive measurement of the specific activity against small chromogenic substrate 4-methylumbelliferyl β-D-cellobioside at 50 °C.[36] (**Figure 4.2**) The extinction coefficient of 48800 $M^{-1}cm^{-1}$ was used to determine the concentration of EGII in solution.[46]

4.2.2 Synthesis of polymethyl acrylic acid (PMAA) coated magnetic nanoparticles : synthesis of MNPs with a core size of ~100 nm, 1.08 g of $FeCl_3 \cdot 6H_2O$, 2.4 g of NaAc and 0.25 g of sodium citrate were dissolved in 20 mL of ethylene glycol. The mixture was stirred vigorously for 0.5 h at room temperature to form a homogeneous dark red solution, transferred into a Teflon-lined stainless-steel autoclave (50 mL capacity) and incubated at 200 ^{o}C for 20 h. The black product was washed with ethanol and separated from the solvent by using a magnet. The washing and separation steps were repeated for several times.

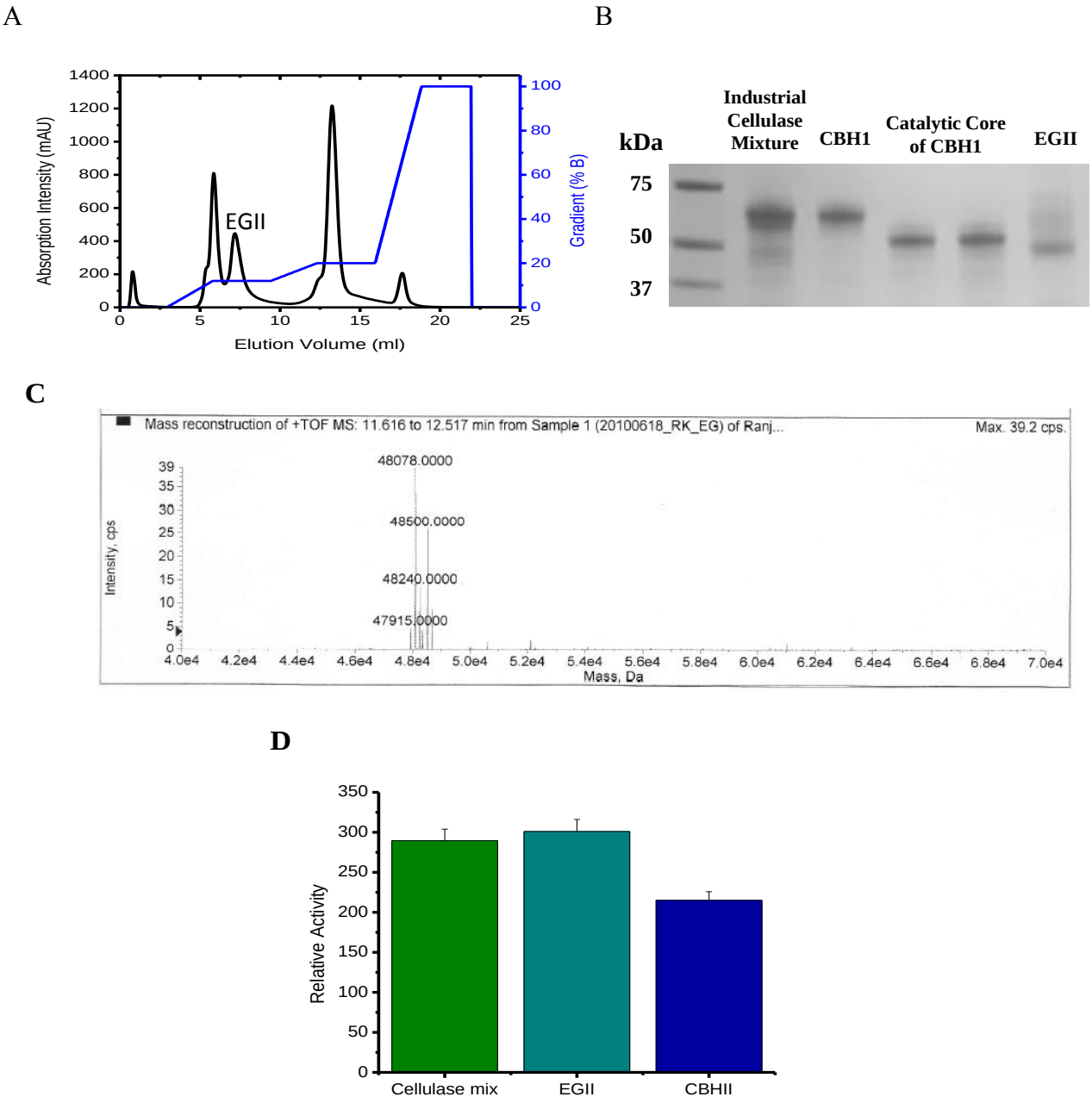

Figure 4.2: (A): FPLC chromatogram of commercial cellulase enzymes. The sample was applied on a Resourse Q column in 20 mM Tris–HCl buffer at pH 8 and eluted by a two-step gradient as indicated in the Figure. (100% B = 100mM NaCl). (B) The molecular

weight of the purified enzymes as determined by SDS-PAGE. (C) Molecular weight determination of EGII using Mass Spectroscopy. (D) Relative specific activities of enzymes against 4-Methylumbelliferyl β-D-cellobioside at 50°C for 10 mins.

To achieve uniform shell thickness, MNPs were modified by MPS before the polymerization step. Modification of MNPs with MPS was achieved by adding 40 mL of ethanol, 10 mL of deionized water, 1.5 mL of $NH_3 \cdot H_2O$ and 0.3 g of MPS into the MNPs ethanol suspension and vigorously stirring the mixture for 24 h at 60 ^oC. The obtained product was separated by using a magnet and washed with ethanol to remove excess MPS. The resultant MNP-MPS nanoparticles were dried in a vacuum oven at 40 ^oC till constant weight. Coating PMAA layer onto MNP-MPS nanoparticles was performed by distillation-precipitation polymerization of MAA in acetonitrile, with MBA as the cross-linker and AIBN as the initiator. Typically, 200 mg of MNP-MPS seed nanoparticles were dispersed in 160 mL acetonitrile in a dried 250 mL single-necked flask, and sonicated for 10 min. A mixture of 0.8 mL of MAA, 89 mg of MBA and 20 mg of AIBN were added to the flask to initiate the polymerization. The flask was submerged in a heating oil bath, and attached with a fractionating column, Liebig condenser, and a receiver. The reaction mixture was heated from ambient temperature to the boiling state within 30 min and the reaction was ended after about 80 mL of acetonitrile was distilled from the reaction mixture (in about 1 h). The MNP-PMAA were collected by magnetic separation and washed with ethanol to remove excess reactants and the polymer nano-spheres (without a MNP core) from the side reactions.

4.2.3 Conjugation of EGII to MNP-PMAA particles. EGII was conjugated to MNP-PMAA using 1-ethyl-3-(3-dimenthylaminopropyl) carbodiimide hydrochloride (EDC) and *N*-

hydroxysulfosuccinimide (Sulfo-NHS) coupling chemistry.[35] For conjugation, MNP-PMAA solutions were prepared in 0.50M MES buffer at pH 6, with a concentration around 10^{11} particles/ml. 2 mg of EDC and 2 mg Sulfo-NHS were then added into 1 ml of particle suspension, and the solution incubated at room temperature with mixing for 10 min. The activated particles were separated from the solution by a magnetic rack, washed, and added into 2 mg/ml CBHI solution in 12 mM PBS buffer at pH 7.4. The mixture was incubated at room temperature in a rotator for 6 hr followed by washing with 50 mM Sodium Acetate buffer for five times to remove unbound proteins. The concentration of CBHI bound to the particles was calculated by comparing the specific activity against 4-methylumbelliferyl β-D-cellobioside in 50 mM sodium acetate at 50 °C with that of the CBHI solutions with the known concentration. (**Figure 4.3**).

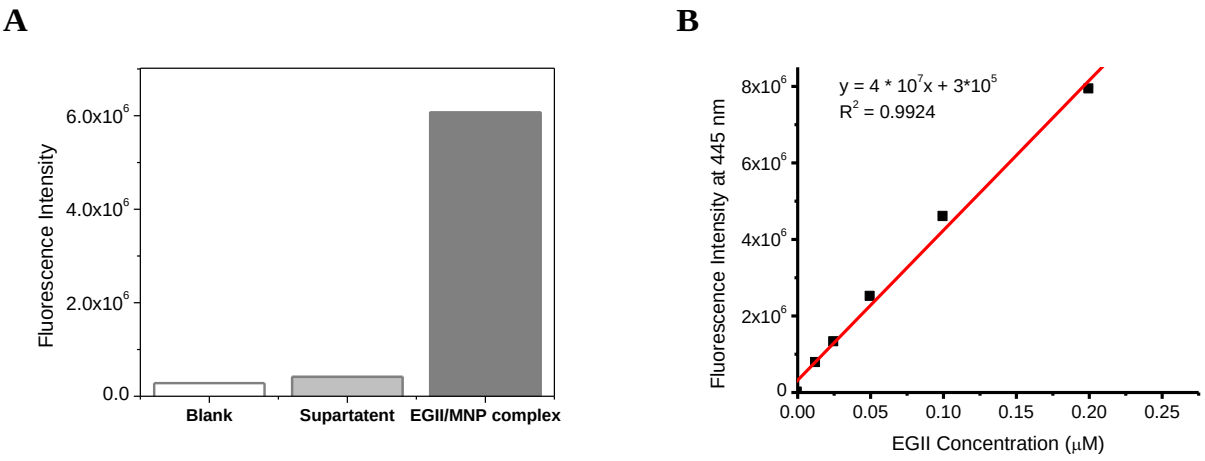

Figure 4.3: (A) Fluorescence intensity of blank, supernatant and EGII/MNP complex solution. Excitation and emission at 365nm and 445nm respectively. (B) Calibration curve of EGII using 4-Methylumbelliferyl β-D-cellobioside at 50°C in 50mM Sodium Acetate

4.2.4 Adsorption and activity experiments for EGII and EGII/MNP-PMAA complexes : For EGII, 1 ml EGII solution in 50 mM Sodium Acetate at pH 6.5 was mixed with 20-60 mg Avicel in a centrifuge tube and incubated at 37°C temperature on a mixer. At given incubation time, the Avicel was pelleted by centrifugation at 14,000 rpm for 3 min and the supernatant was withdrawn. The concentration of unbound EGII in the supernatants was determined by measuring A_{280} and the specific activity against 4-methylumbelliferyl β-D-cellobioside. For EGII /MNP-PMAA, 1 ml EGII /MNP-PMAA solution in 50 mM Sodium Acetate at pH 5 was mixed with 20-60 mg Avicel in a centrifuge tube and incubated at 37°C temperature on a mixer. At given incubation time, a tube was removed from the mixer and put on a rack for 5 min to let the Avicel sediment. Due to their small sizes, the unbound EGII /MNP-PMAA remained fully suspended in solution (up to hours) and were pipetted out to separate unbound enzyme

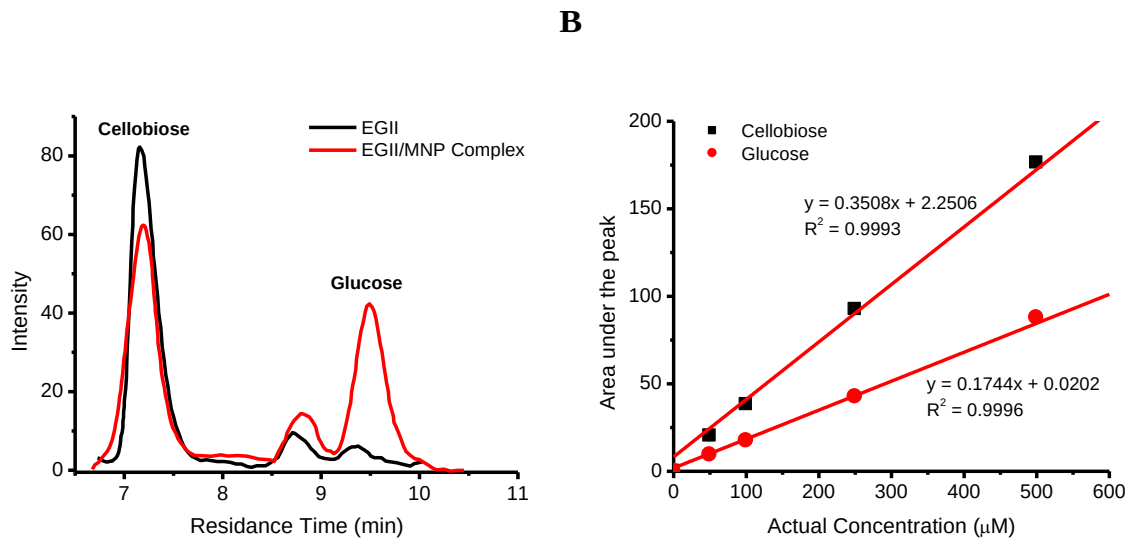

Figure 4.4 : A) Typical HPLC scan of hydrolysis products. Calibration curve of cellobiose and glucose for HPLC analysis.

complexes from the Avicel. The concentration of absorpted EGII complexes on Avicel was then determined by comparing the specific activity against 4-methylumbelliferyl β-D-cellobioside with that of stock solution with predetermined amount of EGII. The suspension of unbounded enzyme complexes or EGII were then pelleted by centrifugation at 14,000 rpm for 3 min and the supernatant was withdrawn to determine the concentration of sugars using HPLC. Adsorption isotherms were determined with 20 mg/ml Avicel. All experiments were done in triplicate

4.2.5 Desorption and surface mobility of EGII complexes on cellulose surface studied by confocal microscopy. The coverslip was placed on a glass slide and affixed by double-side tapes to leave a small gap between the cover slip and the surface of the glass slide. A dilute solution of FITC tagged EGII/MNP-PMAA complexes (~50 μL) with Avicel was then introduced into gap. Before that EGII/MNP complexes where allowed to adsorption on the surface Avicel for 30 mins. Desoprtion and surface mobility of EGII complexes was followed by Nikon A1R spectral confocal microscopy. Sample environment was maintained at a temperature of 37 ± 3 °C using an environmental chamber and images were taken at an interval of 10 minutes. Image analysis was performed by using NIH ImageJ software, and the surface mobility of complexes was analyzed by using CISMM Video Spot Tracker program.

4.3 RESULTS AND DISCUSSION

EGII was purified to homogeneity from industrial cellulases (Novozyme Celluclast) by using GE FPLC AKTA Purifier equipped with ion-exchange columns, and identified based on its molecular weight and its specific activity. The colloidal polymers with a MNP core of 100 nm in diameter and a poly(acrylic acid) (PAA) shell of 30 nm in thickness and 10 % crosslinking (MNP-PAA) were prepared as the scaffold materials by

the method we previously reported.[7] The carboxyl groups of the PAA were then activated for conjugation of EGII by standard carbodiimide coupling chemistry to produce EGII/MNP-PAA complexes. After conjugation, the EGII/MNP-PAA complexes were separated from unbound EGII by a standard magnetic separation rack and washed repeatedly. The system is thus free of interference from freely dispersed enzymes, either before or after their adsorption on the cellulose. The surface densities of EGII on MNP-PAA were measured by an enzymatic assay using 4-methylumbelliferyl-β-D-cellobioside as the fluorescent soluble substrate. EGII/MNP-PAA containing ~200 enzymes per complex (corresponding to 60% coverage of the MNP-PAA surface) were used in the study.

For varying concentrations of EGII/MNP-PAA and EGII, their adsorption to 20 mg/ml Avicel in 50 mM sodium acetate (pH 5) at 37 ˚C and the subsequent hydrolytic reaction were followed (**Figure 4.5)**. The adsorption isotherms are constructed and shown in **Figure 4.6**. The complex concentrations in Figure 2A were determined by dividing the molarity of complexed EGII with the estimated number of EGII per particle. The Langmuir-Freundlich (LF) was used to analyse the adsorption isotherms, as the LF isotherm is able to model the adsorption behaviour of both homogeneous and heterogeneous systems and is suitable for the comparisons of adsorption with very different underlying mechanisms (e.g., in the case of free and complexed EGII). As shown in **Table 4.1**, the apparent binding affinity of EGII/MNP-PAA ($(1.1\pm0.4)*10^{10}$ M^{-1}) is almost six orders of magnitude higher than that of EGII ($(4.6\pm0.02)*10^{4}$ M^{-1}). Such tight binding is attributed to the multivalent interactions between the enzyme complex and the cellulose, and should be irreversible in practice. The maximal binding capacity for

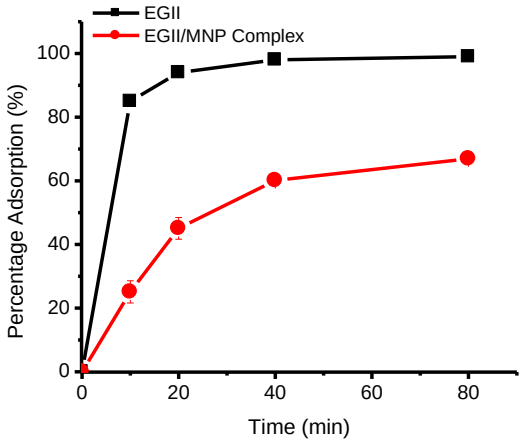

Figure 4.5: Time dependent adsorption of EGII and EGII/MNP complex on cellulose surface. The adsorption was carried out in 50mM Sodium Acetate, pH 5 buffer at 37 °C. The enzyme and avicel concentration was 0.025 µM and 20g/l respectively.

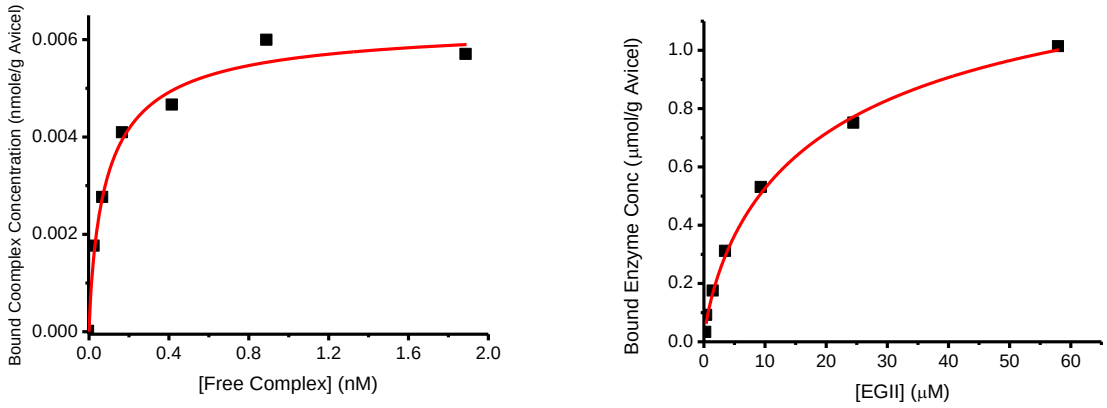

Figure 4.6: Adsorption isothermals of the (A) EGII/MNP-PAA complex and (B) EGII on Avicel. Avicel concentration was kept constant (20 mg/mL), at increasing enzyme concentrations.

EGII/MNP-PAA (0.006 µmol EGII/g Avicel), however, is more than 200 times lower than that of EGII (1.5 µmol EGII/g Avicel). It has been known that cellulosic particles

like Avicel have both external and internal surfaces, and the internal surface area (pores of 1-10 nm in sizes) can be up to 2 orders higher than the external area. Our binding capability result indicates that the intra-particulate pores of Avicel are not accessible to EGII/MNP-PAA with a diameter of 140 ± 20 nm. The diminished accessibility may become a limiting factor to the overall performance of polycatalytic complexes.

Table 4.1: Mean binding affinity, binding capacities and the heterogeneity index for the adsorption of the polycatalytic complexes and the free EGII to Avicel.

Sample	Mean binding affinity (M^{-1})	Binding Capacity (μmol/g Avicel)	Heterogeneity Index
EGII/MNP-PAA	$(1.1 \pm 0.37) \times 10^{10}$	0.0064 ± 0.0006	0.83 ± 0.22
EGII	$(4.6 \pm 0.02) \times 10^{4}$	1.47 ± 0.17	0.76 ± 0.07

Figure 4.7 compares the enzymatic reactions of EGII/MNP-PAA and EGII on Avicel, by measuring the amount of soluble sugars (e.g., cellobiose and glucose) released from Avicel at an identical total enzyme concentration. At higher enzyme-to-cellulose ratio, EGII has better efficiency in the production of soluble sugars than the polycatalytic EGII complexes, but at the lower enzyme-to-cellulose ratios, EGII/MNP-PAA exhibited greater efficiency compared to the EGII. The control experiments on MNP-PAA without enzymes show that the colloidal scaffolds alone do not have hydrolytic activity in degrading cellulose. We note here almost 100% of the EGII adsorbed on the cellulose surface in the different enzyme-to-cellulose ratios examined. But the adsorption levels of EGII complexes strongly depend on the concentration of enzymes and cellulose, due to their low binding capacity (**Table 4.1** and **Figure 4.7**). To compare the inherent activity

in soluble sugar production between EGII and EGII/MNP-PAA complex, we calculated the reaction productivity by normalizing the amount of released soluble sugar after 24 h, according to the actual fraction of enzyme complexes or enzymes bound on the cellulose.

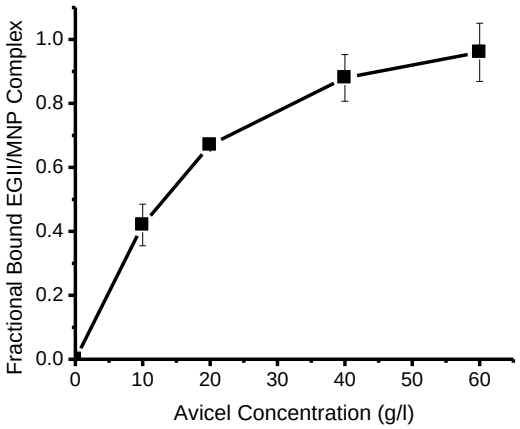

Figure 4.7: Fractional adsorption of EGII/MNP complexes on cellulose with increasing substrate concentration. The total enzyme concentration was kept constant at 0.025 μM. The avicel concentration was varied from 10 – 60 g/l.

Figure 4.8 shows that, after correction, EGII/MNP-PAA has significantly higher productivity than the EGII at the examined enzyme concentrations. The enhanced substrate interaction and succeeding attacks from multiple enzymes in the EGII complexes seem to improve their capability in producing soluble sugars. The overall performance of EGII complexes, however, is limited by their low binding capability to cellulose as they cannot access to the internal surface of Avicel.

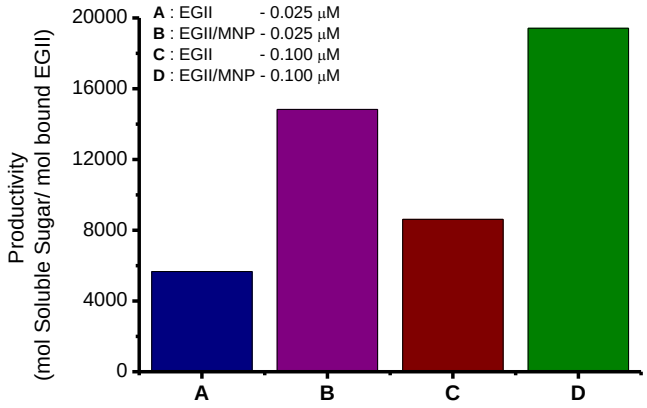

Figure 4.8: Productivity values of EGII and EGII/MNP complexes at different total enzyme concentration.

The sugar production patterns were considerably different between complexed and free EGII. The proportion of the produced sugars (e.g., cellobiose vs. glucose) for EGII/MNP-PAA was rather independent of both the enzyme-to-substrate ratios and the time of hydrolysis (**Figure 4.9A-B**), with glucose as the major product. In contrast, EGII produced more cellobiose than glucose at low enzyme-to-substrate ratios (**Figure 4.9C-D**). Only at much higher enzyme loading, glucose became the dominant soluble products (**Figure 4.9E-F**), as also found in the prior studies.[8] The exact mechanisms for production of soluble sugars by EGII, an endoglucanase, are still not very clear. But our result suggests that the formation of polycatalytic complexes that anchor on the cellulose substrate and possess many enzymes in the close proximity may enhance the prospect of having continuing, multiple attacks on cellulose chains and further digesting cellooligosaccharides to glucose. The collective actions of multiple enzymes in the complexes should facilitate the distinct reaction activities and product patterns.

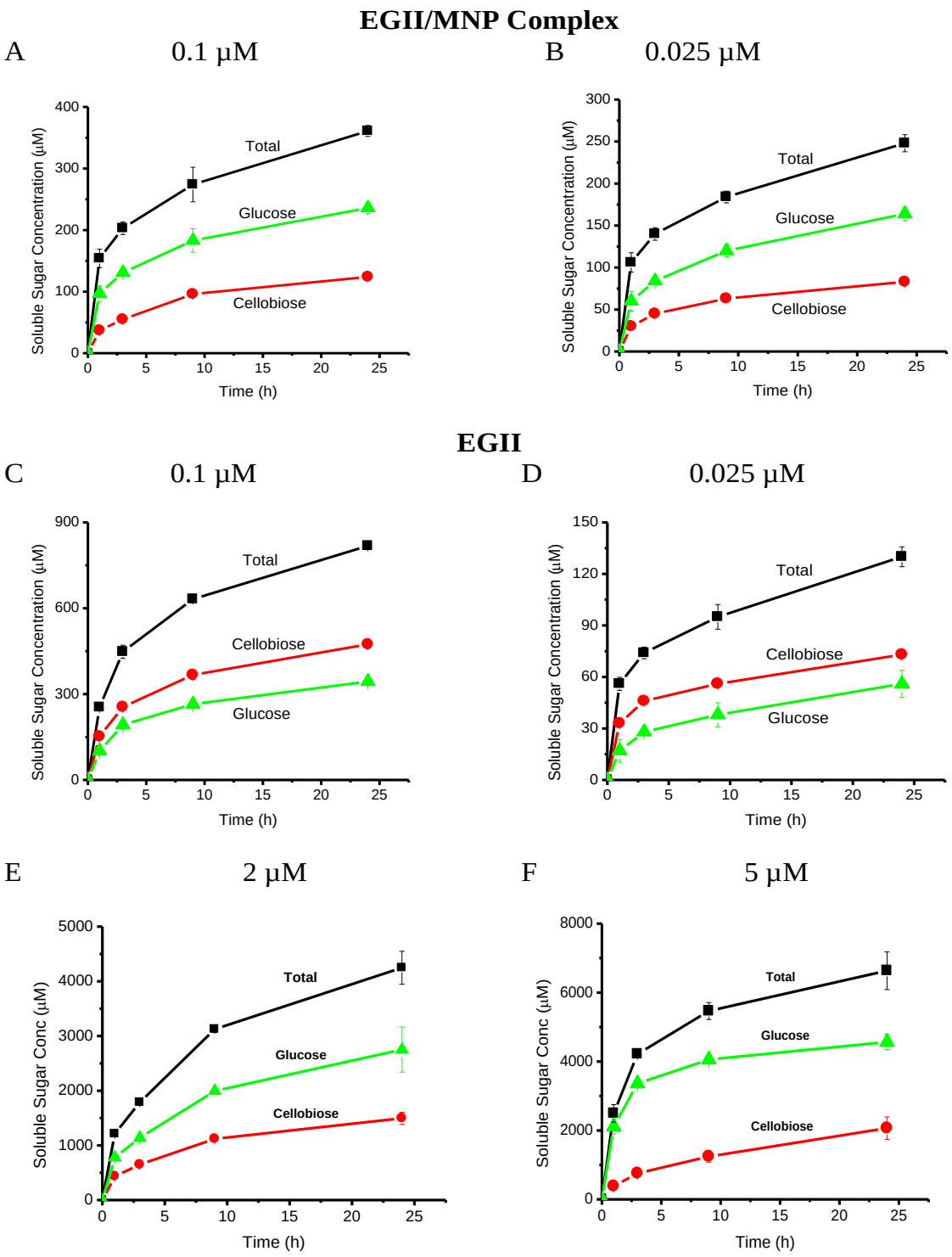

Figure 4.9: Hydrolysis kinetics of Avicel by EGII in the free state (A & B) and EGII/MNP-PAA complex (C - F). Initial concentrations of total enzymes and Avicel are as indicated. Incubation was at 37 ˚C in 50 mM sodium acetate, pH 5.

We then used laser-scanning fluorescence confocal microscopy (LFCM) to follow the adsorption and motions of individual EGII complexes on Avicel cellulose, to confirm our findings derived from the experiments based on ensemble behaviour. EGII/MNP-PAA complexes were conjugated with fluorescein isothiocyanate (FITC) for fluorescence imaging and introduced into the buffer solution containing Avicel particles. The adsorption and desorption of individual complexes can be readily followed using time-lapse imaging (**Figure 4.10**). Our study shows that once bounded, the EGII complexes rarely desorpted in the time scale of the experiments (~1 h). This is in agreement with the high binding affinity we measured for the polycatalytic complexes

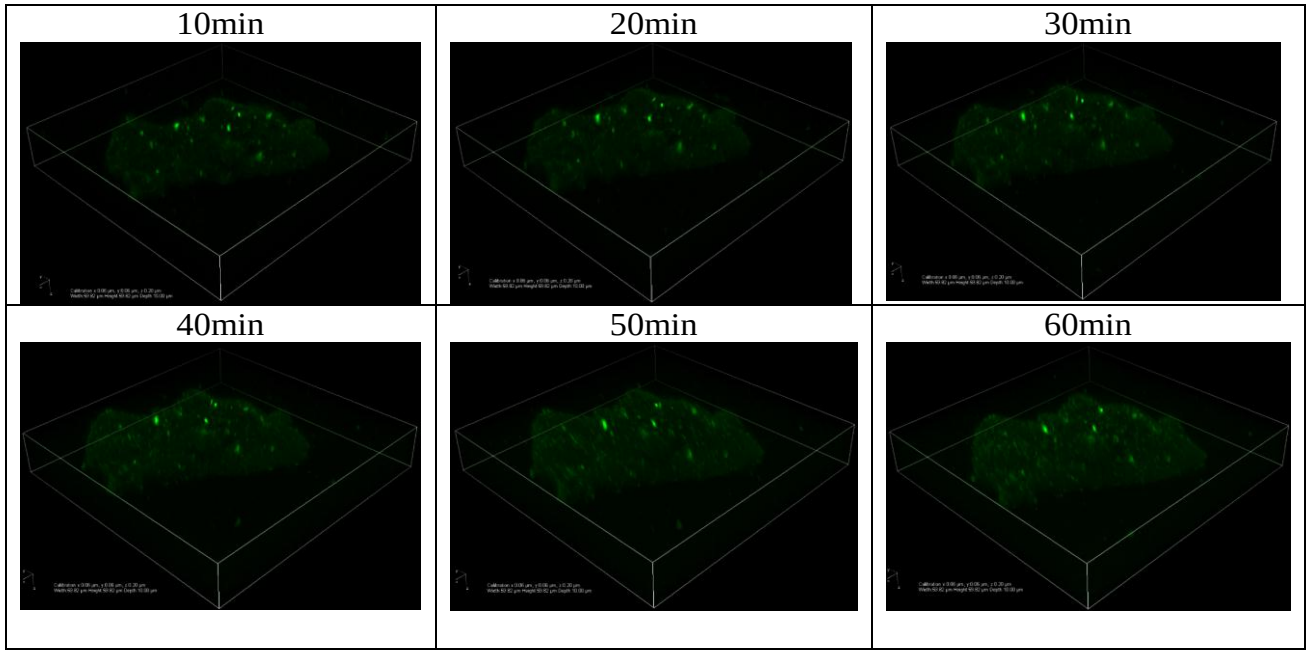

Figure 4.10: Time-dependent LFCM study on the desorption of EGII/MNP-PAA complexes on the Avicel cellulose. The experiment was performed in 50 mM sodium acetate buffer, pH 5, at 37 ˚C. The images have a size of 60nm/pixel.

The coverage of EGII complexes on Avicel was further revealed by the Field Emission Scanning Electron Microscopy (FESEM) study (**Figure 4.11**) on the samples. Interestingly, the hydrolytic reaction of EGII/MNP-PAA complexes generated cavities at their anchoring sites, which can be visualized after merely 2 hours of incubation. It also suggests that the complexes, as a whole, do not possess much lateral mobility on the cellulose substrate.

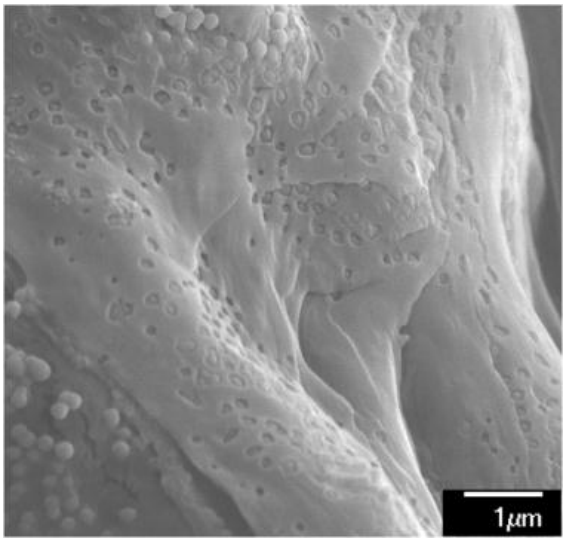

Figure 4.11: FESEM image of Avicel incubated with EGII/MNP-PAA complexes for 2 hrs in 50 mM sodium acetate buffer, pH 5, at 37 ˚C.

In summary, we developed EGII based artificial polycatalytic cellulase complexes and compared its adsorption and activity with freely floating EGII. We observed that, although, artificial cellulase complexes are inherently more active but they are unable to compete with natural cellulase at higher concentration due to its large size and very strong binding. So the progress in developing economical biofuel will not only depend on

improving the activity of cellulase but also promoting its accessibility and mobility on cellulose surface.

REFERENCES

1. S.-Y. Ding, Y.-S. Liu, Y. Zeng, M. E. Himmel, J. O. Baker and E. A. Bayer, *Science (Washington, DC, U. S.)*, **2012**, 338, 1055-1060.
2. B. Nidetzky, W. Steiner and M. Claeyssens, *Biochem J*, **1994**, 303 **(Pt 3)**, 817-823.
3. K. Igarashi, T. Uchihashi, A. Koivula, M. Wada, S. Kimura, T. Okamoto, M. Penttilae, T. Ando and M. Samejima, *Science (Washington, DC, U. S.)*, **2011**, 333, 1279-1282.
4. E. J. Cho, S. Jung, H. J. Kim, Y. G. Lee, K. C. Nam, H.-J. Lee and H.-J. Bae, *Chem. Commun. (Cambridge, U. K.)*, **2012**, 48, 886-888.
5. R. K. Kamat, W. Ma, Y. Yang, Y. Zhang, C. Wang, C. V. Kumar and Y. Lin, *ACS Appl. Mater. Interfaces*, **2013**, 5, 8486-8494.
6. D.-M. Kim, M. Umetsu, K. Takai, T. Matsuyama, N. Ishida, H. Takahashi, R. Asano and I. Kumagai, *Small*, **2011**, 7, 656-664.
7. W. Ma, S. Xu, J. Li, J. Guo, Y. Lin and C. Wang, *J. Polym. Sci., Part A: Polym. Chem.*, **2011**, 49, 2725-2733.

Chapter 5

Summary and Future Directions

4.1 Summary

Biomass is a sustainable and renewable energy resource that can be converted to liquid transportation fuels. However, conversion of cellulosic biomass into fuels is challenging due to its recalcitrant nature for enzymatic degradation. Inspired by the high efficiency of natural polycatalytic cellulase complex, cellulosome, we aim *to create and investigate artificial cellulosomes with high activity, and systematically evaluate the fundamental principles that underlie their structure, dynamics and catalytic functions.*

We first studied the free cellulase system and observed unique change in enzyme kinetics above certain enzyme/substrate ratio. Analysis of enzyme kinetics, processivity and turnover number indicates that formation of on-site assembly on cellulose surface helps it to overcome obstacle and regain processivity which causes the change in enzymatic activity. This study clearly indicates that free enzymes also uses complex form to enhance its activity. This finding will help us to identify critical parameters required in a highly efficient artificial cellulase complex.

In order to understand how adsorption, diffusion and activity of fungal cellulase changes on complex formation, we first developed a polycatalytic system consisting of cellulases covalently linked on the surface of colloidal polymers with a magnetic nanoparticle (MNP) core. MNP provides a convenient handle to separate the complex, while the colloidal polymer would serve as a benign scaffold to attach the enzymes. The formation of polycatalytic complex increases the rate of hydrolytic reactions on cellulose, but only at relatively low enzyme/substrate ratios. At

these conditions, the free enzymes are prone to get stuck on the cellulose surface and lost their processivity. The polycatalytic complexes, instead, works very efficiently even at very low enzyme concentration due to high local molarity of enzymes. However, once bounded, the polycatalytic complexes can only carry out reactions locally and not capable of relocating to new sites, due to their lack of long-range surface mobility and their extremely small dissociation constants. Therefore, at increased enzyme/substrate ratios, free enzymes gradually become more effective, presumably with the help of a cooperative mechanism that regains the processivity of trapped enzyme. Surface mobility of CBHI complex was measured by TIRF microscopy and analyzed using video tracking software. CBHI complex shows no long range mobility on cellulose surface which contributed to certain extent in its lower activity at high enzyme concentration. We also identified the effect of scaffold size and polymer shell type on the adsorption and activity of CBHI complex.

Biochemical properties of EGII based complexes were also similar to CBHI complexes i.e. it shows higher activity than free EGII at lower concentration but at higher concentration free EGII showed better activity. Our adsorption and surface mobility study indicated that lack of accessibility and mobility of EGII complexes on cellulose surface lead to lower activity at higher concentration. Thus development of polycatalytic cellulase complexes for efficient conversion of biomass into biofuel will not only depends on improving the activity of cellulase but also on improving its accessibility and mobility on cellulose surface.

4.2 Future Directions

The present studies clearly show the significant effect of complex formation on the biochemical properties of cellulase enzymes. The cellulase complex developed in the present study shows

significantly higher activity than free cellulase but only in certain enzyme/substrate ratio. At higher enzyme/substrate ratio, due to its spherical morphology, lack of surface mobility and accessibility on cellulose surface lead to poor activity. Thus, the opportunity in the development of highly optimized polycatalytic complexes across different concentration ranges may come from the design of new nano-scaffolds that can indeed coordinate the motions of individual enzymes in the complex, and that can couple the external forces to gain motility to speed up the overall enzymatic reactions. So based on present study, in order to develop artificial cellulosome complex with high efficiency we need to investigate following factors on adsorption, diffusion and activity of cellulase complex;

1. Effect of scaffold architecture.

2. Effect of surface rigidity of nanoparticle.

3. Orientation of enzyme on scaffold surface.

It will be also interesting to develop brush polymer having multiple chain ends which can be used to conjugates cellulase. The polymer scaffold will allow all enzymes to bind to the substrate surface and perform catalytic reaction which is the major drawbacks of spherical scaffold. We believe systematic study of artificial cellulase complex like the present study will help us to improve the enzymatic depolymerization of cellulose and make biofuel economically feasible.